Advanced Engineering Informatics 48 (2021) 101299

Contents lists available at ScienceDirect

Advanced Engineering Informatics

journal homepage: www.elsevier.com/locate/aei

An integrated optimization method for tactical-level planning in liner shipping with heterogeneous ship fleet and environmental considerations

Junayed Pasha [a], Maxim A. Dulebenets [b,*], Amir M. Fathollahi-Fard [c], Guangdong Tian [d], Yui-yip Lau [e], Prashant Singh [a], Benbu Liang [f]

[a] Department of Civil & Environmental Engineering, Florida A&M University-Florida State University (FAMU-FSU) College of Engineering, 2525 Pottsdamer Street, Building B, Suite B339, Tallahassee, FL 32310-6046, USA
[b] Department of Civil & Environmental Engineering, Florida A&M University-Florida State University (FAMU-FSU) College of Engineering, 2525 Pottsdamer Street, Building A, Suite A124, Tallahassee, FL 32310-6046, USA
[c] Department of Electrical Engineering, École de Technologie Supérieure, University of Quebec, 1100 Notre-Dame St. W., Montreal, Quebec, Canada
[d] School of Mechanical Engineering, Shandong University, Jinan 250061, China
[e] Division of Business and Hospitality Management, College of Professional and Continuing Education, The Hong Kong Polytechnic University
[f] School of Management, Wuhan University of Technology, Wuhan 430070, China

ARTICLE INFO

Keywords:
Liner shipping
Heterogeneous fleet
Service frequency determination
Ship fleet deployment
Sailing speed optimization
Ship scheduling

ABSTRACT

The maritime transportation flows and container demand have been increasing over time, although the COVID-19 pandemic may slow down this trend for some time. One of the common strategies adopted by shipping lines to efficiently serve the existing customers is the deployment of large ships. The current practice in the liner shipping industry is to deploy a combination of ships of different types with different carrying capacities (i.e., heterogeneous fleet), especially at the routes with a significant demand. However, heterogeneous fleets of ships have been investigated by a very few studies addressing the tactical liner shipping decisions (i.e., determination of service frequency, ship fleet deployment, optimization of ship sailing speed, and design of ship schedules). Moreover, limited research efforts have been carried out to simultaneously capture all the major tactical liner shipping decisions using a single solution methodology. Therefore, this study proposes an integrated optimization model that addresses all the major tactical liner shipping decisions and allows the deployment of a heterogeneous ship fleet at each route, considering emissions generated throughout liner shipping operations. The model's objective maximizes the total turnaround profit generated from liner shipping operations. A decomposition-based heuristic algorithm is presented in this study to solve the model proposed and efficiently tackle large-size problem instances. Numerical experiments, carried out for a number of real-world liner shipping routes, demonstrate the effectiveness of the proposed methodology. A set of managerial insights, obtained from the proposed methodology, are also provided.

1. Background

Shipping lines encounter a number of challenges throughout planning of their operations [1,2]. One of these challenges is the continuous growth in container demand, since more and more companies are outsourcing their operations and moving their production activities offshore. However, the COVID-19 pandemic may slow down this trend in container demand for some time. In order to address the demand growth and efficiently serve the existing diverse customers, shipping lines have adopted various strategies (e.g., formation of alliances, operations optimization, deployment of large ships). One of the common strategies is the deployment of large ships. The largest container ships in the world now have capacities close to 24,000 twenty-foot equivalent units (TEUs), as compared to the capacity of 500–1,000 TEUs that was common in 1956 [3,4]. Large ships assist shipping lines with economies of scale, savings in fuel consumption, emission reduction, and lower transportation cost per unit [5]. Due to economies of scale, large ships enable shipping lines to reduce freight rates and effectively share the

* Corresponding author.
E-mail addresses: jp17j@my.fsu.edu (J. Pasha), mdulebenets@eng.famu.fsu.edu (M.A. Dulebenets), amirmohammad.fathollahifard.1@ens.etsmtl.ca (A.M. Fathollahi-Fard), tiangd2013@163.com (G. Tian), yuiyip.lau@cpce-polyu.edu.hk (Y.-y. Lau), prashant1.singh@famu.edu (P. Singh), liangbenbu@whut.edu.cn (B. Liang).

https://doi.org/10.1016/j.aei.2021.101299
Received 8 January 2021; Received in revised form 4 April 2021; Accepted 15 April 2021
1474-0346/© 2021 Elsevier Ltd. All rights reserved.

existing capacity with other shipping lines [6].

However, some disadvantages are associated with large ships, such as port congestion, extensive pressure on marine container terminals (MCTs) as well as inland operators, unused ship capacity, among others. Still, shipping lines are replacing small ships with large ones. Many shipping lines use a combination of large, medium, and small ships (i.e., heterogeneous fleet) along certain routes (a.k.a., port rotations), especially at the routes with a significant demand. For instance, the French Asia Line 1 route served by the CMA-CGM shipping line is covered by the ships with capacities ranging between 14,812 TEUs and 20,954 TEUs as of August 2020 [7]. In fact, most of the Asia-Europe routes served by the CMA-CGM shipping line have heterogeneous fleets of ships. The other major shipping lines, such as OOCL, Maersk, MSC, COSCO, Evergreen, also deploy heterogeneous fleets along many routes.

Even though shipping lines deploy heterogeneous fleets of ships along many service routes, a significant proportion of the liner shipping literature, especially the ones addressing the tactical liner shipping decisions, assume the deployment of a homogeneous fleet of ships along a given service route. Such an assumption has significant disadvantages for real-world scenarios, where shipping lines tend to deploy heterogeneous fleets. The homogeneous ship fleet models do not allow capturing certain important operational features, such as: (1) extra fees charged by port operators for large ships due to the use of specific air/water drafts, advanced container handling equipment, larger storage spaces, etc. [6]; (2) higher cost of operation for large ships, such as crew, repair and maintenance, docking, and insurance [5]; (3) higher cost of fuel consumption for large ships [8]; (4) higher capacity of large ships that can be used to accommodate the demand from alliance partners; and others. Hence, the mathematical models, addressing the tactical liner shipping decisions, should directly account for the deployment of heterogeneous fleets of ships.

The main tactical liner shipping decisions include: (i) determination of service frequency; (ii) ship fleet deployment; (iii) optimization of ship sailing speed; and (iv) design of ship schedules. Many studies focusing on the aforementioned decisions have been conducted to date [1,9]. Some of these decisions overlap with each other (e.g., the ship sailing speed optimization models and the ship schedule design models both determine the ship sailing speed). However, there are some distinct differences between these decisions as well. For instance, the ship sailing speed optimization models may capture certain environmental considerations but generally ignore the service of ships at ports. On the other hand, the ship schedule design models explicitly capture the service of ships at ports but may ignore the environmental considerations. Furthermore, the canonical ship schedule design models do not assign ship types to routes, and this decision is strictly determined at the ship fleet deployment stage [1,9].

The service frequency refers to the time interval between consecutive ship visits at a port of call. Lam and Voorde [10] indicated that maintaining the common practice of weekly service frequency, when interconnected with unreliability in ship schedules, could lead to difficulties associated with timely production and distribution. Tai and Lin [11] assessed the impact of daily service frequency and slow steaming on emissions generated from liner shipping. It was found that the daily frequency could reduce emissions, even when the strategy of slow steaming was not adopted. The study that was conducted by Lin and Tsai [12] outlined different aspects of daily service frequency. Zhang and Lam [13] examined the Daily Maersk service that adopted the daily service frequency as well. Giovannini and Psaraftis [14] integrated the determination of service frequency with the design of ship schedules. The study assessed the variable service frequency with the aim of maximizing the total profit.

The ship fleet deployment problem, on the other hand, deals with the assignment of ships to routes. Moura et al. [15] studied the assignment of a heterogeneous fleet of ships in a hub-and-spoke environment. An integer formulation was developed in the study to minimize the total annual trade cost. Results from the executed computational experiments favored to assign a small fleet of ships. Álvarez [16] studied the fleet deployment and routing of container ships. For a short-term ship fleet deployment, Meng and Wang [17] devised a chance-constrained model that considered container demand uncertainty. In order to model container demand uncertainty, the study assumed a normal distribution of container demand among two consecutive ports under a given route. Gelareh and Pisinger [18] presented an optimization model for the problem of simultaneous ship fleet deployment and network design. A methodology for repositioning of empty containers, while addressing the fleet deployment, was proposed by Huang et al. [19]. Zheng et al. [20] proposed a network design model for liner shipping alliances, which accounted for the ship fleet deployment decisions. Since the proposed model was for liner shipping alliances, the carrying capacities of ships were exchanged between different alliance partners. Several other aspects were integrated as well, such as container routing and variable container demand. Thun et al. [21] tackled the network design problem and considered assigning one type of ship to each liner shipping route. The study promoted multiple visits to a single port of call in order to incorporate various route structures. During the numerical experiments, however, a maximum of two visits were allowed for a port to reduce the CPU time.

The optimization of ship sailing speed is a critical decision, as it substantially affects the total route service cost. A number of studies on optimization of ship sailing speed have investigated changes in the ship fuel consumption, since fuel consumption is a major predictor of ship sailing speed [22,23]. Ronen [22] found that by decreasing ship sailing speed by only 20%, fuel consumption could be reduced to 50%. Throughout optimization of ship sailing speed, transshipment as well as routing of freight containers were addressed by Wang and Meng [24]. Kim [25] presented an optimization-based method to determine the ship sailing speed for every voyage leg, while selecting refueling ports for ships as well. A Lagrangian heuristic was developed and used as a solution method. A set of experiments, which employed the data from real-world practices, liner shipping literature, and random generation, evaluated the performance of the proposed approach. Wang and Meng [23] assessed the difference between real speed and planned speed of ships. Mander [26] asserted that slow steaming was one of the most popular methods in liner shipping that could lead to environmental sustainability. Cheaitou and Cariou [27] contemplated the container demand as elastic, and it varied with the ship sailing speed. Zhao et al. [28] assessed a loss aversion mechanism for slow steaming and analyzed tradeoffs between delays in delivery, emissions, along with fuel consumption. A Genetic Algorithm with special operators was developed to tackle the proposed mathematical model.

The design of ship schedules covers a wide array of decisions regarding port waiting times, arrival times, departure times, sailing times, and so on. This is the most complicated of the problems at the tactical-level planning of liner shipping. Qi and Song [29] assessed uncertainties in port times and considered ship sailing speed constraints. While capturing uncertainties in port times, Song et al. [30] determined the required quantity of ships, ship sailing speeds, and ship schedules. Several studies modeled the availability of multiple handling rates (HRs) at ports and/or availability of multiple port arrival time windows (TWs) throughout scheduling of ships [31–34]. Wang [35] acknowledged the fact that the capacities of ships, allocated to serve a given route, might vary. The study proposed some rules for the optimal ship sequencing in a string. Gürel and Shadmand [36] studied the design of ship schedules, while addressing uncertainties in port handling times and waiting times. The study also facilitated heterogeneous fleets of ships, which involved different fuel consumption functions for different types of ships. Ozcan et al. [37] designed ship schedules, while addressing the cargo allocation problem and considering transshipment operations and transit times. Zhang et al. [38] studied the design of ship schedules for a two-way tidal channel, whose depth was impacted by tides. Zhuge et al. [39] reported that a number of ports adopted voluntary speed reduction initiatives. Hence, the study examined ship schedules under such

initiatives.

For broader surveys of the literature on liner shipping, ship fleet deployment, and design of ship schedules, this study refers the readers to Meng et al. [1], Wang and Meng [40], and Dulebenets et al. [9]. Among the existing ship scheduling studies, only a few efforts captured a heterogeneous nature of the ship fleet [5,35,36]. In the meantime, only one study, conducted by Pasha et al. [41], captured all the major tactical liner shipping decisions (i.e., determination of service frequency, ship fleet deployment, optimization of ship sailing speed, and design of ship schedules). However, the model, which was proposed by Pasha et al. [41], assigned a homogeneous fleet of ships to every route. Hence, there is a need for more studies that can capture all the major tactical liner shipping decisions, as integrated solution methodologies could effectively assist shipping lines with operations planning. At the same time, the mathematical models that allow allocation of heterogeneous ship fleets are also required to capture shipping behavior that is common for many routes. Taking into consideration the aforementioned state-of-the-art gaps, the present study offers the following contributions:

- This study proposes a mathematical model, which encompasses all the major tactical liner shipping decisions (i.e., determination of service frequency, ship fleet deployment, optimization of ship sailing speed, and design of ship schedules).
- Unlike the majority of the existing liner shipping models, the mathematical model, developed in this study, allows the deployment of a heterogeneous ship fleet at each route.
- In order to support environmental sustainability, the developed model penalizes the quantity of emissions generated due to hauling of ships in sea and due to container handling at ports.
- Considering the computational complexity of the proposed optimization model, a novel decomposition-based heuristic algorithm is presented in this study to solve the model and efficiently tackle large-size problem instances.
- A set of comprehensive experiments are performed to demonstrate the effectiveness of the decomposition-based heuristic algorithm developed and showcase some managerial implications using the integrated optimization model proposed.

The remainder of this manuscript is composed of the following sections. The next section contains a detailed description of the problem addressed in this study, while the third section formulates the proposed optimization model for integrated tactical liner shipping decisions with heterogeneous ship fleet and environmental considerations. The fourth section demonstrates the developed solution approach. The fifth section conducts the numerical experiments, and the final section provides some concluding remarks.

2. Problem description

This study directly accounts for each one of the main tactical liner shipping decisions that a shipping line has to address. A full description of the tackled problem in a comprehensive manner is given in this section, which captures the main features of liner shipping, such as: (1) liner shipping routes; (2) fleet of ships; (3) service of ships at ports; (4) container demand sensitivity; (5) frequency of service; (6) ship sailing speed; (7) fuel consumption; (8) container inventory; (9) liner shipping emissions; and (10) objective of a shipping line. Note that a detailed description of all the sets, parameters, and variables (decision and auxiliary variables), which were adopted in the problem description and the model formulation proposed, are provided in Appendix A for the ease of reference. All the decision and auxiliary variables will be denoted using a bold font, while the parameters will be listed in a standard font.

2.1. Liner shipping routes

A shipping line generally operates on a number of routes. Let $R = \{1, \cdots, n^1\}$ be the set of routes or port rotations (i.e., the sequence of ports that are visited by a ship). The number of ports of call is usually different for different routes. Let $P_r = \{1, \cdots, n_r^2\}, r \in R$ denote the set of ports for liner shipping route r. Three hypothetical routes for liner shipping, each consisting of four ports of call, are illustrated in Fig. 1. Every route begins and ends at a specific port (e.g., Gavle, Norrkoping, and Grangemouth in routes "1", "2", and "3", respectively). A port may be called or visited multiple times within one rotation. However, the port indices for different visits at a port should be different. In route "1", Gdynia is visited twice in one round trip. For the first visit (after visiting Gavle), its port index is "2", while the port index for Gdynia is set to "4" for the second visit (after calling Gdansk). Furthermore, a port may be under more than one liner shipping route. For example, Norrkoping is covered by liner shipping routes "1" and "2". Note that the ship schedules (e.g., sailing time, arrival time, waiting time, departure time) are fixed for every port under a given route. The pathway between two successive ports (e.g., port p and port $p + 1$) is called a voyage leg (e.g., voyage leg p). For instance, liner shipping route "1" includes five voyage legs.

2.2. Fleet of ships

Depending on the type, ships have various carrying capacities, engine configurations, fuel consumption rates, etc. Therefore, the associated costs may vary based on the ship type. However, ships of a given type generally have the same mechanical attributes, such as fuel consumption rate, maximum hauling speed, emissions generated, among others. This assumption is applied by most of the studies addressing the ship scheduling problem and the ship fleet deployment problem, even though it may not hold true for all the scenarios due to age of ships, previous maintenance activities, utilization frequency, along with other operational factors [40]. In order to maximize the overall profit or to minimize the overall cost, a shipping line takes decisions on what type of ships to assign to a liner shipping route from the available types of ships ($V = \{1, \cdots, n^3\}$). Whether all the ports under a liner shipping route can handle a given type of ship also affects the ship fleet deployment decisions, which is directly captured by the following inequality:

$$\boldsymbol{d}_{rv} \leq d_{rv}^0 \forall r \in R, v \in V \tag{1}$$

where:

$\boldsymbol{d}_{rv}$ – is 1 if ship type v is deployed for service of liner shipping route r (=0 otherwise);

d_{rv}^0 – is 1 if type v ships can be deployed for service of liner shipping route r (=0 otherwise).

Note that this study allows allocation of multiple types of ships to each liner shipping route (i.e., deployment of a heterogeneous ship fleet), which is a common practice among shipping lines, especially at the routes with a significant demand. Each shipping line has a limited quantity of ships of a given type in its fleet ($q_v^{own-m}, v \in V$ – ships). When q_v^{own-m} is lower than the required quantity of ships of type v to be assigned to liner shipping route r, the shipping line may have to charter ships from other shipping lines. In that case, an additional chartering cost ($c_v^{char}, v \in V$ – USD per day) is to be remunerated.

2.3. Service of ships at ports

Ships can arrive at ports during the arrival TWs offered by the MCT operators of the respective ports of call. Denote $T_{rp} = \{1, \cdots, n_{rp}^4\}, r \in R, p \in P_r$ as the set of arrival TWs available at port p of liner shipping route r. The TWs start and end at the previously specified times, which are established based negotiations between the MCT operators and shipping lines. This study takes into account early and late ship arrivals at ports

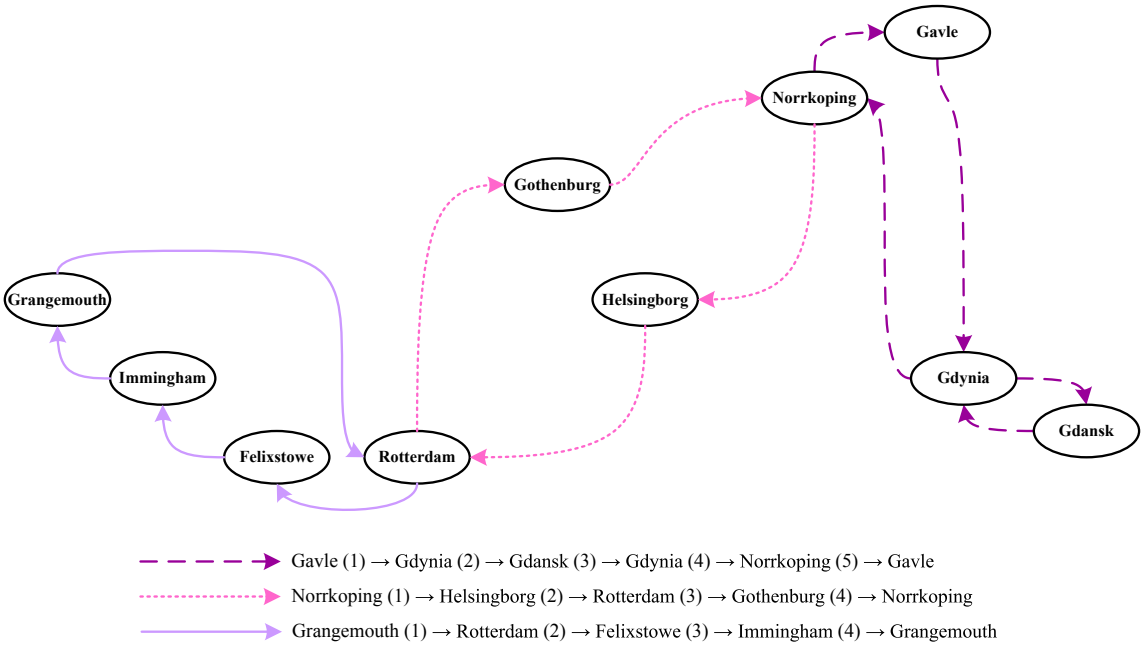

Fig. 1. Hypothetical routes for liner shipping.

before the start and after the end of the arrival TWs, respectively (i.e., the soft time window concept). If the ships arrive early, no charge is imposed. However, in case of a late arrival, the shipping line has to pay a cost of late arrivals ($\boldsymbol{LAC}$ – USD), which can be calculated from the following relationship:

$$\boldsymbol{LAC} = \sum_{r\in R}\sum_{p\in P_r} c_{rp}^{late} \cdot \boldsymbol{\tau}_{rp}^{late} \tag{2}$$

where:

$\boldsymbol{\tau}_{rp}^{late}, r \in R, p \in P_r$ – is the late arrival time of a ship for port p of liner shipping route r (hours);

$c_{rp}^{late}, r \in R, p \in P_r$ – is the unit cost of late arrivals for port p of liner shipping route r (USD per hour).

Under each arrival TW, several HRs ($H_{rpt} = \left\{1, \cdots, n_{rpt}^{5}\right\}, r \in R, p \in P_r, t \in T_{rp}$) are provided by the MCT operators. A handling productivity ($ph_{rpth}, r \in R, p \in P_r, t \in T_{rp}, h \in H_{rpt}$ – TEUs per hour) is associated with each HR. If the shipping line decides to select an HR with a high handling productivity, the ship handling time ($\boldsymbol{\tau}_{rpth}^{hand}, r \in R, p \in P_r, t \in T_{rp}, h \in H_{rpt}$ – hours) would be reduced, which would further lead to savings in fuel consumption, as the ships would be able to spend more time in sea (by sailing at a lower speed) due to savings in handling time. However, if the shipping line decides to select the HRs with the highest handling productivity at each port, such an action may not be practical from the economic perspective. In particular, selecting an HR with a high handling productivity would lead to a high cost of container handling at ports ($c_{rpthv}^{hand}, r \in R, p \in P_r, t \in T_{rp}, h \in H_{rpt}, v \in V$ – USD per TEU) that would be imposed to the shipping line, as more resources would have to be used by the MCT operators for serving the arriving ships. The cost of container handling at ports could also be high for large ships, since advanced handling equipment, large storage space, and specific water/air drafts are required for large ships [5].

2.4. Container demand sensitivity

When the ship sailing speed is higher, some customers prefer to transport a larger amount of cargo. Hence, this study makes an assumption that the amount of containers that are handled at ports ($\boldsymbol{QC}_{rp}^{PORT}, r \in R, p \in P_r$ – TEUs) is elastic and depends on ship sailing speeds, which is in line with some of the previously conducted efforts on liner shipping [27,41]. The mathematical formulation for the elastic container demand can then be expressed as follows:

$$\boldsymbol{QC}_{rp}^{PORT} = \alpha_{rp}^{dem} - \frac{\beta_{rp}^{dem}}{\boldsymbol{\vartheta}_{rp}} \forall r \in R, p \in P_r \tag{3}$$

where:

$\alpha_{rp}^{dem}, \beta_{rp}^{dem}, r \in R, p \in P_r$ – are the coefficients that describe sensitivity of container demand;

$\boldsymbol{\vartheta}_{rp}, r \in R, p \in P_r$ – is the ship sailing speed along voyage leg p for liner shipping route r (knots).

Upon arrival at a port, the MCT operator offloads the import containers and loads the export containers to the ship. Thus, the amount of containers transported along the voyage legs ($\boldsymbol{QC}_{rpv}^{SEA}, r \in R, p \in P_r, v \in V$ – TEUs) can be calculated as follows:

$$\boldsymbol{QC}_{r(p+1)v}^{SEA} = \boldsymbol{QC}_{rpv}^{SEA} - \boldsymbol{QC}_{r(p+1)}^{PORT} \cdot Import_{r(p+1)} + \boldsymbol{QC}_{r(p+1)}^{PORT} \cdot \left(1 - Import_{r(p+1)}\right) \forall r \in R,$$

$$p \in P_r, p < n_r^2, v \in V \tag{4}$$

$$\boldsymbol{QC}_{r(1)v}^{SEA} = QC_{rv}^{SEA-0} - \boldsymbol{QC}_{r(1)}^{PORT} \cdot Import_{r(1)} + \boldsymbol{QC}_{r(1)}^{PORT} \cdot \left(1 - Import_{r(1)}\right) \forall r \in R, v \in V \tag{5}$$

where:

$Import_{rp}, r \in R, p \in P_r$ – is the proportion of import containers at port p of liner shipping route r;

$QC_{rv}^{SEA-0}, r \in R, v \in V$ – is the total amount of containers on a type v ship before the ship is docked at the first port for liner shipping route r (TEUs).

Note that the index "v" has been added in terms $\boldsymbol{QC}_{rpv}^{SEA}, r \in R, p \in P_r, v \in V$ and $QC_{rv}^{SEA-0}, r \in R, v \in V$ to capture the effects of ship heterogeneity (i.e., different ship types are likely to carry different amounts of containers along the voyage legs for a given liner shipping route due to the differences in ship capacities).

2.5. Frequency of service

The following relationship should be ensured by the shipping line to maintain the frequency of service, which is a period between subsequent ship arrivals at a port [31]:

$$24 \cdot \boldsymbol{\phi}_r \cdot \boldsymbol{q}_r = \sum_{p \in P_r} \boldsymbol{\tau}_{rp}^{sail} + \sum_{p \in P_r} \sum_{t \in T_{rp}} \sum_{h \in H_{rpt}} \boldsymbol{\tau}_{rpth}^{hand} \cdot \boldsymbol{x}_{rpth} + \sum_{p \in P_r} \boldsymbol{\tau}_{rp}^{wait} \forall r \in R \quad (6)$$

where:

24 – is the conversion factor from days to hours;

$\boldsymbol{\phi}_r, r \in R$ – is the frequency of port service for liner shipping route r (days);

$\boldsymbol{q}_r, r \in R$ – is the total quantity of ships required for liner shipping route r (ships);

$\boldsymbol{\tau}_{rp}^{sail}, r \in R, p \in P_r$ – is the sailing time of a ship at voyage leg p of liner shipping route r (hours);

$\boldsymbol{x}_{rpth}, r \in R, p \in P_r, t \in T_{rp}, h \in H_{rpt}$ – is 1 if HR h is selected by the shipping line at port p of liner shipping route r during TW t (=0 otherwise);

$\boldsymbol{\tau}_{rp}^{wait}, r \in R, p \in P_r$ – is the waiting time of a ship at port p of liner shipping route r (hours).

The ships, required for deployment at a liner shipping route, can be from the shipping line's fleet and/or chartered from the fleets of other shipping lines. In case of chartering, a chartering cost should be paid, which is generally higher than the operating cost for the same type of ships. The required quantity of ships for a liner shipping route, the total cost of ship operating (***SOC*** – USD), and the total cost of ship chartering (***SCC*** – USD) can be estimated as follows:

$$\boldsymbol{q}_r = \sum_{v \in V} \left(\boldsymbol{q}_{rv}^{own} + \boldsymbol{q}_{rv}^{char} \right) \forall r \in R \quad (7)$$

$$\boldsymbol{SOC} = \sum_{r \in R} \sum_{v \in V} c_v^{oper} \cdot \boldsymbol{q}_{rv}^{own} \cdot \boldsymbol{\phi}_r \quad (8)$$

$$\boldsymbol{SCC} = \sum_{r \in R} \sum_{v \in V} c_v^{char} \cdot \boldsymbol{q}_{rv}^{char} \cdot \boldsymbol{\phi}_r \quad (9)$$

where:

$\boldsymbol{q}_{rv}^{own}, r \in R, v \in V$ – is the quantity of ships of type v in the shipping line's own fleet assigned to liner shipping route r (ships);

$\boldsymbol{q}_{rv}^{char}, r \in R, v \in V$ – is the quantity of chartered ships of type v assigned to liner shipping route r (ships);

$c_v^{oper}, v \in V$ – is the unit cost of ship operating (USD per day).

2.6. Ship sailing speed

The ship sailing speed, along with the length of the voyage leg ($l_{rp}, r \in R, p \in P_r$ – nmi), determines the ship sailing time as follows:

$$\boldsymbol{\tau}_{rp}^{sail} = \frac{l_{rp}}{\boldsymbol{\vartheta}_{rp}} \forall r \in R, p \in P_r \quad (10)$$

The shipping line has to make several considerations to set the ship sailing speed for a voyage leg of a given liner shipping route. The lower bound on the ship sailing speed is generally set to reduce the deterioration of the ship engines [42]. The upper bound, on the other hand, is mostly influenced by engine capacities [8]. Several other factors affect ship sailing speeds, such as transit time of ships, unit cost of emissions, unit cost of fuel, unit cost of ship operating, unit cost of inventory, etc. Decreasing the ship sailing speed reduces the fuel consumption along with the emissions generated in sea. However, it will increase the total container transit time in sea, and, therefore, will necessitate the deployment of more ships in order to maintain the frequency of service, which will ultimately increase the cost of ship operating or chartering. At the same time, reducing the ship sailing speed to a certain level may cause violation of the requirements imposed on the transit time. For selecting ship sailing speeds for different types of ships, this study supports the following theorem.

Theorem 1. *In order to maintain the target frequency of service at every port of call for a given liner shipping route, a shipping line should select the same ship sailing speed along a given voyage leg for all types of ships.*

Proof. Let's assume a shipping line has two types of ships $v^1, v^2 \in V$ for deployment at liner shipping route $r \in R$. At first, a type v^1 ship arrives at port p_r, offloads/loads cargo, and then leaves for port $(p+1)_r$, which is situated at a distance of l_{rp} from port p_r (see Fig. 2). If the shipping line decides to haul the type v^1 ship at a speed of ϑ_{rp}^1 along voyage leg p_r, the ship will arrive at port $(p+1)_r$ at time $\tau_{r(p+1)}^{arr} = \tau_{rp}^{dep} + l_{rp}/\vartheta_{rp}^1$, where τ_{rp}^{dep} is the departure time from port p_r. Later on, a type v^2 ship travels from port p_r to port $(p+1)_r$. If type v^2 ships are smaller than type v^1 ships, then, the shipping line would be able to haul the type v^2 ship along voyage leg p_r at speed $\vartheta_{rp}^2 > \vartheta_{rp}^1$ with no surge in fuel consumption (as smaller ships generally consume less fuel per nautical mile). In such a case, the type v^2 ship will arrive at port $(p+1)_r$ at time $\tau_{r(p+1)}^{\widehat{arr}} = \tau_{rp}^{dep} + l_{rp}/\vartheta_{rp}^2$, which is earlier than $\tau_{r(p+1)}^{arr}$. Since $\tau_{r(p+1)}^{\widehat{arr}} \neq \tau_{r(p+1)}^{arr}$, the service frequency at port $(p+1)_r$ will be violated. Therefore, a uniform ship sailing speed $\vartheta_{rp} = \vartheta_{rp}^1 = \vartheta_{rp}^2$ must be selected along voyage leg p_r for all types of ships in order to comply with the service frequency requirements. □

2.7. Fuel consumption

Several factors directly influence the fuel consumption function of a ship engine, such as ship sailing speed, payload, weather conditions, depth of water, and the geometric features of a ship [24,33,43]. Wang and Meng [24] reported that the ship sailing speed is the most influential predictor of fuel consumption of the main ship engines that move the propellers. The design fuel consumption ($f_{rpv}^{design}, r \in R, p \in P_r, v \in V$ – tons per nmi) can be quantified from the following power-law relationship [33,43]:

$$f_{rpv}^{design} = \frac{\gamma_v \cdot \left(\vartheta_{rp} \right)^{(\alpha_v - 1)}}{24} \forall r \in R, p \in P_r, v \in V \quad (11)$$

where:

$\alpha_v, \gamma_v, v \in V$ – are the coefficients that describe the behavior of fuel consumption function for type v ships.

Several contemporary studies on liner shipping argue that the ship payload is one of the principal variables affecting the fuel consumption rate [41,43,44]. Hence, the final fuel consumption rate ($f_{rpv}, r \in R, p \in P_r, v \in V$ – tons per nmi) will be estimated considering the payload supported by ships [41,45]:

$$\begin{aligned} f_{rpv} &= f_{rpv}^{design} \cdot \left(\frac{\boldsymbol{QC}_{rpv}^{SEA} \cdot AWC + LWT_v}{TWC_v + LWT_v} \right)^{\frac{2}{3}} \\ &= \frac{\gamma_v \cdot \left(\vartheta_{rp} \right)^{(\alpha_v - 1)}}{24} \cdot \left(\frac{\boldsymbol{QC}_{rpv}^{SEA} \cdot AWC + LWT_v}{TWC_v + LWT_v} \right)^{\frac{2}{3}} \end{aligned} \quad (12)$$

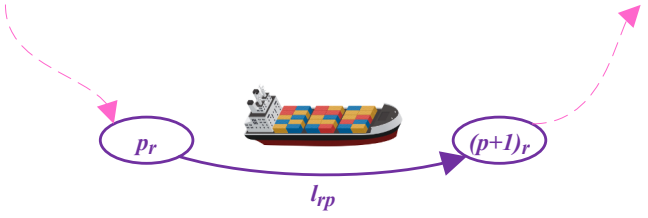

Fig. 2. Voyage between two ports of call.

$\forall r \in R, p \in P_r, v \in V$

where:

AWC – is the average cargo weight within a typical 20-ft container (tons);

$LWT_v, v \in V$ – is the empty weight of a ship of type v (tons);

$TWC_v, v \in V$ – is the total carrying capacity of a ship of type v (tons).

Note that the design fuel consumption as well as the final fuel consumption could be different for different types of ships, as indicated by the index "v". Factors that influence the ship sailing speed during a voyage (such as wind speed, wave height, and peak wave period) are not accounted for in this research but could be incorporated as a part of the future works, as additional data would be required to model the effects of these factors on ship fuel consumption. Furthermore, the fuel consumption cost of auxiliary ship engines (i.e., engines providing power on board) is included under the cost of ship operating or chartering.

2.8. Container inventory

The cost of inventory in sea is typically greater than the cost of inventory at ports. This is because the cost of inventory in sea is correlated with the total sailing time of a ship carrying containers at the voyage legs. The cost of inventory at ports, on the contrary, is correlated with the total waiting time as well as the container handling time at ports. The sum of the waiting and handling time at ports is typically smaller than the sailing time of ships along the voyage legs, which makes the cost of inventory at ports less than its counterpart in sea. These costs can be estimated as follows [41]:

$$\boldsymbol{CIC}^{SEA} = c^{inv} \cdot \sum_{r\in R}\sum_{p\in P_r}\sum_{v\in V} \boldsymbol{QC}^{SEA}_{rpv} \cdot \boldsymbol{\tau}^{sail}_{rp} \tag{13}$$

$$\boldsymbol{CIC}^{PORT} = c^{inv} \cdot \sum_{r\in R}\sum_{p\in P_r}\sum_{v\in V} \boldsymbol{QC}^{SEA}_{rpv} \cdot \boldsymbol{\tau}^{wait}_{rp} + c^{inv} \cdot \sum_{r\in R}\sum_{p\in P_r}\sum_{t\in T_{rp}}\sum_{h\in H_{rpt}}\sum_{v\in V} \left(\boldsymbol{QC}^{SEA}_{rpv} - \boldsymbol{QC}^{PORT}_{rp}\right) \cdot \boldsymbol{\tau}^{hand}_{rpth} \cdot \boldsymbol{x}_{rpth} \tag{14}$$

where:

$\boldsymbol{CIC}^{SEA}$ – is the total cost of inventory in sea (USD);

c^{inv} – is the unit cost of inventory (USD per TEU per hour);

$\boldsymbol{CIC}^{PORT}$ – is the total cost of inventory at ports (USD).

2.9. Liner shipping emissions

The quantity of emissions to be produced by a type v ship at voyage leg p of liner shipping route r ($\boldsymbol{EP}^{SEA}_{rpv}, r \in R, p \in P_r, v \in V$ – tons) is dependent on the emission factor in sea (EF^{SEA} – tons of emissions per ton of fuel) along with the ship fuel consumption, and it can be calculated as follows [43]:

$$\boldsymbol{EP}^{SEA}_{rpv} = EF^{SEA} \cdot l_{rp} \cdot \boldsymbol{f}_{rpv} \forall r \in R, p \in P_r, v \in V \tag{15}$$

The quantity of emissions to be generated at ports is correlated with the emission factor at ports and the amount of containers that are handled at ports. Besides, the quantity of emissions to be generated at ports is influenced by the handling productivity, since the handling productivity is correlated with the amount and/or type of handling equipment to be used for ship service at a port. The quantity of emissions generated due to container handling for a type v ship at port p of liner shipping route r ($\boldsymbol{EP}^{PORT}_{rpv}, r \in R, p \in P_r, v \in V$ – tons) can be quantified using the emission factor at ports ($EF^{PORT}_{rphv}, r \in R, p \in P_r, h \in H_{rpt}, v \in V$ – tons of emissions per TEU) as follows [46]:

$$\boldsymbol{EP}^{PORT}_{rpv} = \boldsymbol{QC}^{PORT}_{rp} \cdot \sum_{t\in T_{rp}}\sum_{h\in H_{rpt}} (EF^{PORT}_{rphv} \cdot \boldsymbol{x}_{rpth}) \forall r \in R, p \in P_r, v \in V \tag{16}$$

The methodology for estimation of emissions/cost of emissions, employed by this study, could be potentially used to model the main pollutants generated from oceangoing ships (e.g., CO_2, NO_x, SO_x). The total cost of emissions due to hauling of ships in sea ($\boldsymbol{EC}^{SEA}$ – USD) and the total cost of emissions due to container handling at ports ($\boldsymbol{EC}^{PORT}$ – USD) are correlated with the unit cost of emissions (c^{emis} – USD per ton), and these costs can be estimated as follows:

$$\boldsymbol{EC}^{SEA} = c^{emis} \cdot \sum_{r\in R}\sum_{p\in P_r}\sum_{v\in V} \boldsymbol{EP}^{SEA}_{rpv} \tag{17}$$

$$\boldsymbol{EC}^{PORT} = c^{emis} \cdot \sum_{r\in R}\sum_{p\in P_r}\sum_{v\in V} \boldsymbol{EP}^{PORT}_{rpv} \tag{18}$$

2.10. Objective of a shipping line

The utmost objective of a shipping line is to maximize its total profit that can be represented as a difference between the total revenue generated from its service and the total cost (i.e., sum of all the costs incurred throughout container shipping operations). A significant portion of the mathematical models addressing the tactical liner shipping decisions, especially the ship scheduling models, use the total route service cost in their objective functions [9,31]. This study, however, uses the total turnaround cost in the objective function of its mathematical model, as heterogeneous fleets of ships are facilitated by this study. For heterogeneous fleets of ships, the total route service cost may fluctuate throughout the journey of deployed ships. For instance, if a larger ship is sailing along the voyage leg that requires a specific ship sailing speed, the fuel consumption as well as the associated fuel cost would be higher as compared to the next week, when a smaller ship could sail along the same voyage leg. When selecting the objective function for a shipping line with heterogeneous ship fleets, this study supports the following theorem:

Theorem 2. *Minimizing the total cost of route service for the tactical liner shipping decisions with heterogeneous ship fleets may not be an appropriate objective function, as the total cost of route service could fluctuate throughout the journey of deployed ships.*

Proof. Let's consider the example illustrated in Fig. 3, where the shipping line covers only one liner shipping route with two ports (i.e., $n^1_l = 1$; $n^2_l = 2$). All the major tactical-level decisions are determined for these ports. The service frequency is set to seven days (i.e., $\phi_l = 7$). At port "1", the ships are served under TW "1" and HR "1" with a handling time of τ^{hand}_{1111} (=30 hours). Then, they sail to port "2" at a speed of ϑ_{11} (=15 knots) for a duration of τ^{sail}_{11} (=150 hours). At port "2", the ships are served under TW "2" and HR "2" with a handling time of τ^{hand}_{1222} (=36 hours). Then, they sail back to port "1" at a speed of ϑ_{12} (=20 knots) for a duration of τ^{sail}_{12} (=120 hours). Thus, the total turnaround time is $30+150+36+120 = 336$ hours. To maintain the target service frequency of seven days, the shipping line would need $336/(24 \cdot 7) = 2$ ships. For simplicity, this example would assume only two of the total route service cost components, namely the total cost of ship operating and the total cost of fuel consumption. Moreover, the final fuel consumption rate (f_{rpv}) will be assumed to be equal to the design fuel consumption rate (f^{design}_{rpv}). The aforementioned cost components can be estimated for both homogeneous and heterogeneous fleets of ships, as described below.

Scenario 1: Homogeneous Fleet

In this scenario, two ships of type "1" are deployed, which have the following properties: $c^{oper}_1 = 35{,}000$ USD per day; $\alpha_1 = 3.0$; $\gamma_1 = 0.012$ (see Fig. 3a). The unit cost of fuel is $c^{fuel} = 200$ USD/ton [41]. Then, the total cost of ship operating ($\boldsymbol{SOC}^1$) and the total cost of fuel consumption ($\boldsymbol{FCC}^1$) for scenario 1 can be estimated as follows:

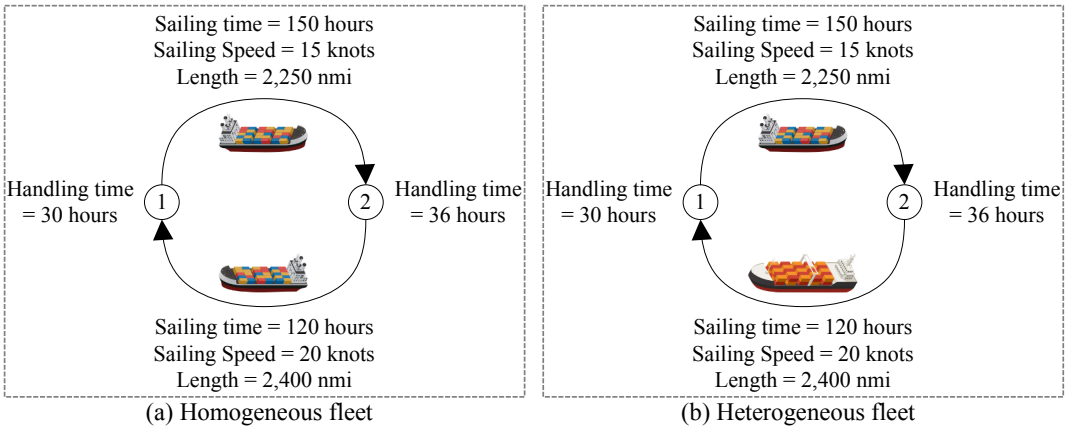

Fig. 3. A liner shipping route with two ports of call.

$$\boldsymbol{SOC}^1 = \sum_{r\in R}\sum_{v\in V} c_v^{oper} \cdot \boldsymbol{q}_{rv}^{own} \cdot \boldsymbol{\phi}_r = 35,000 \cdot 2 \cdot 7 = 490,000 \text{ USD}.$$

$$\begin{aligned}\boldsymbol{FCC}^1 &= c^{fuel} \cdot \sum_{r\in R}\sum_{p\in P_r}\sum_{v\in V} l_{rp} \cdot \frac{\gamma_v \cdot \left(\boldsymbol{\vartheta}_{rp}\right)^{(\alpha_v-1)}}{24} \\ &= 200 \cdot \left(2,250 \cdot \frac{0.012 \cdot 15^{(3.0-1)}}{24} + 2,400 \cdot \frac{0.012 \cdot 20^{(3.0-1)}}{24}\right) \\ &= 146,625 \text{ USD}.\end{aligned}$$

Thus, the total route service cost would be $490,000 + 146,625 = 636,625$ USD, and it will remain the same for all weeks.

Scenario 2: Heterogeneous Fleet

In this scenario, one ship of type "1" and one ship of type "2" will be deployed (see Fig. 3b). Type "2" ships have the following properties: $c_2^{oper} = 43{,}000$ USD per day; $\alpha_2 = 3.2$; $\gamma_2 = 0.014$ [41]. In week 1, the type "1" ship will sail along voyage leg "1", and the type "2" ship will sail along voyage leg "2". In week 2, the type "2" ship will sail along voyage leg "1", and the type "1" ship will sail along voyage leg "2". Then, the total costs of ship operating for weeks 1 and 2 ($\boldsymbol{SOC}_1^2$ and $\boldsymbol{SOC}_2^2$) and the total costs of fuel consumption for weeks 1 and 2 ($\boldsymbol{FCC}_1^2$ and $\boldsymbol{FCC}_2^2$) for scenario 2 can be estimated as follows:

Week 1:

$$\begin{aligned}\boldsymbol{SOC}_1^2 &= \sum_{r\in R}\sum_{v\in V} c_v^{oper} \cdot \boldsymbol{q}_{rv}^{own} \cdot \boldsymbol{\phi}_r = 35,000 \cdot 1 \cdot 7 + 43,000 \cdot 1 \cdot 7 \\ &= 546,000 \text{ USD}.\end{aligned}$$

$$\begin{aligned}\boldsymbol{FCC}_1^2 &= c^{fuel} \cdot \sum_{r\in R}\sum_{p\in P_r}\sum_{v\in V} l_{rp} \cdot \frac{\gamma_v \cdot \left(\boldsymbol{\vartheta}_{rp}\right)^{(\alpha_v-1)}}{24} \\ &= 200 \cdot \left(2,250 \cdot \frac{0.012 \cdot 15^{(3.0-1)}}{24} + 2,400 \cdot \frac{0.014 \cdot 20^{(3.2-1)}}{24}\right) \\ &= 254,528 \text{ USD}.\end{aligned}$$

The total route service cost, incurred by the shipping line during week 1, would be $546,000 + 254,528 = 800,528$ USD.

Week 2:

$$\begin{aligned}\boldsymbol{SOC}_2^2 &= \sum_{r\in R}\sum_{v\in V} c_v^{oper} \cdot \boldsymbol{q}_{rv}^{own} \cdot \boldsymbol{\phi}_r = 43,000 \cdot 1 \cdot 7 + 35,000 \cdot 1 \cdot 7 \\ &= 546,000 \text{ USD}.\end{aligned}$$

$$\begin{aligned}\boldsymbol{FCC}_2^2 &= c^{fuel} \cdot \sum_{r\in R}\sum_{p\in P_r}\sum_{v\in V} l_{rp} \cdot \frac{\gamma_v \cdot \left(\boldsymbol{\vartheta}_{rp}\right)^{(\alpha_v-1)}}{24} \\ &= 200 \cdot \left(2,250 \cdot \frac{0.014 \cdot 15^{(3.2-1)}}{24} + 2,400 \cdot \frac{0.012 \cdot 20^{(3.0-1)}}{24}\right) \\ &= 197,515 \text{ USD}.\end{aligned}$$

The total route service cost, incurred by the shipping line during week 2, would be $546,000 + 197,515 = 743,515$ USD.

Based on the provided example, it can be noticed that the total cost of route service is different for different weeks in case of heterogeneous ship fleets. Therefore, the total route service cost may fluctuate throughout the journey of deployed ships for the routes that are served by heterogeneous ship fleets. □

The total turnaround cost, on the other hand, represents the summation of all the costs that are incurred by each one of the ships in the fleet throughout the round journey (i.e., departure from the first port of call, visit of all the consecutive ports of the route, and return to the first port of call). In the presented example, the total turnaround cost is $800,528 + 743,515 = 1,544,043$ USD, and it will remain the same throughout the journey of deployed ships. In order to estimate the total turnaround cost components, which will be used in the objective function of the optimization model under study, the associated total route service cost components will be multiplied with the term $(\boldsymbol{q}_{rv}^{own} + \boldsymbol{q}_{rv}^{char})$.

3. Optimization model

The Integrated Optimization Model for Tactical-Level Planning Decisions in Liner Shipping with Heterogeneous Ship Fleet and Environmental Considerations (**TLP-HSF**) is presented in this section of the manuscript. First, some linearization techniques that were deployed to reduce the **TLP-HSF** computational complexity are described. Then, a mathematical formulation for the **TLP-HSF** optimization model is provided. Note that all the tactical-level planning decisions in the proposed **TLP-HSF** mathematical model are to be made by the shipping line, not by other relevant stakeholders (e.g., MCT operators, shippers, alliance partners, etc.).

3.1. Reduction of nonlinearity

A set of commonly used linearization techniques are employed in this study to decrease the degree of nonlinearity of the mathematical formulation proposed. Particularly, the ship sailing speed ($\boldsymbol{\vartheta}_{rp}, r \in R, p \in P_r$ – knots) will be removed from the model, and its reciprocal $\boldsymbol{y}_{rp} = \frac{1}{\boldsymbol{\vartheta}_{rp}} \forall r \in R, p \in P_r$ (knots^{-1}) will be used instead. Moreover, the design fuel consumption function $f_{rpv}^{design}, r \in R, p \in P_r, v \in V$ will

be linearized using a piecewise linear approximation. $S_v = \{1, \cdots, n_v^6\}$, $v \in V$ will be further used to denote the set of linear segments used in the piecewise linear approximation of fuel consumption. For each one of the linear segments, the design fuel consumption will be estimated. It was found that using four or more linear segments in the linear approximation of fuel consumption generated the results close to the nonlinear fuel consumption function (see Fig. 4 where γ_v was assumed to be 0.012, while α_v was assumed to be 3.0). Hence, four linear segments in the linear approximation of fuel consumption will be used throughout this study for each ship type.

3.2. Mathematical formulation

In the **TLP-HSF** optimization model, the shipping line intends to maximize the total turnaround profit (19), which depends on the total turnaround revenue along with the total turnaround cost that consists of: (a) the total cost of ship operating; (b) the total cost of ship chartering; (c) the total cost of container handling at ports; (d) the total cost of late arrivals; (e) the total cost of fuel consumption; (f) the total cost of inventory in sea as well as at ports; and (g) the total cost of emissions in sea as well as at ports.

$$max\left[\boldsymbol{REV} - \left(\boldsymbol{SOC} + \boldsymbol{SCC} + \boldsymbol{PHC} + \boldsymbol{LAC} + \boldsymbol{FCC} + \boldsymbol{CIC}^{SEA} + \boldsymbol{CIC}^{PORT} + \boldsymbol{EC}^{SEA} + \boldsymbol{EC}^{PORT}\right)\right] \tag{19}$$

A set of operational constraints are imposed within the **TLP-HSF** optimization model to capture the main tactical-level features of liner shipping planning. More specifically, the **TLP-HSF** optimization model has a total of seven groups of constraints. The first group of constraints [i.e., constraints (20)-(22)] imposes some operational requirements regarding the selection of arrival TWs and HRs for the ships at each port under each liner shipping route. In particular, constraints (20) ensure that the shipping line will select a single arrival TW for each port under each liner shipping route. Constraints (21) guarantee that a single HR will be selected for each port. Constraints (22) ensure that the handling rate that was selected will be used during the chosen arrival TW for each port under each liner shipping route.

$$\sum_{t \in T_{rp}} \boldsymbol{z}_{rpt} = 1 \forall r \in R, p \in P_r \tag{20}$$

$$\sum_{t \in T_{rp}} \sum_{h \in H_{rpt}} \boldsymbol{x}_{rpth} = 1 \forall r \in R, p \in P_r \tag{21}$$

$$\boldsymbol{x}_{rpth} \le \boldsymbol{z}_{rpt} \forall r \in R, p \in P_r, t \in T_{rp}, h \in H_{rpt} \tag{22}$$

The second group of constraints computes the container demand based on the reciprocal of ship sailing speed [i.e., constraints (23)] and the amount of containers on each ship deployed for service of ports [i.e., constraints (24)-(26)].

$$\boldsymbol{QC}_{rp}^{PORT} = \alpha_{rp}^{dem} - \boldsymbol{y}_{rp} \cdot \beta_{rp}^{dem} \forall r \in R, p \in P_r \tag{23}$$

$$\boldsymbol{QC}_{r(p+1)v}^{SEA} = \boldsymbol{QC}_{rpv}^{SEA} - \boldsymbol{QC}_{r(p+1)}^{PORT} \cdot Import_{r(p+1)} + \boldsymbol{QC}_{r(p+1)}^{PORT} \cdot \left(1 - Import_{r(p+1)}\right) \forall r \in R,$$

$$p \in P_r, p < n_r^2, v \in V \tag{24}$$

$$\boldsymbol{QC}_{r(1)v}^{SEA} = QC_{rv}^{SEA-0} - \boldsymbol{QC}_{r(1)}^{PORT} \cdot Import_{r(1)} + \boldsymbol{QC}_{r(1)}^{PORT} \cdot \left(1 - Import_{r(1)}\right) \forall r \in R, v \in V \tag{25}$$

$$\boldsymbol{QC}_{rpv}^{sea} \cdot AWC \le TWC_v + M_1 \cdot (1 - \boldsymbol{d}_{rv}) \forall r \in R, p \in P_r, v \in V \tag{26}$$

The third group of constraints [i.e., constraints (27)-(32)] focuses on estimations of the ship sailing speed along with fuel consumption for each voyage leg of each liner shipping route. More specifically, constraints (27) and (28) guarantee that the ship sailing speed will not exceed the pre-determined range at each voyage leg. Constraints (29) guarantee that a single linear segment will be chosen for the function that is used to calculate the approximated fuel consumption at a given voyage leg. Constraints (30) and (31) ensure that the appropriate linear segment will be chosen based on the ship sailing speed reciprocal values. Constraints (32) estimate the fuel consumption using the linear segment that was selected.

$$\frac{1}{\vartheta^{max}} \le \boldsymbol{y}_{rp} \forall r \in R, p \in P_r \tag{27}$$

$$\boldsymbol{y}_{rp} \le \frac{1}{\vartheta^{min}} \forall r \in R, p \in P_r \tag{28}$$

$$\sum_{s \in S_v} \boldsymbol{g}_{rps} = 1 \forall r \in R, p \in P_r \tag{29}$$

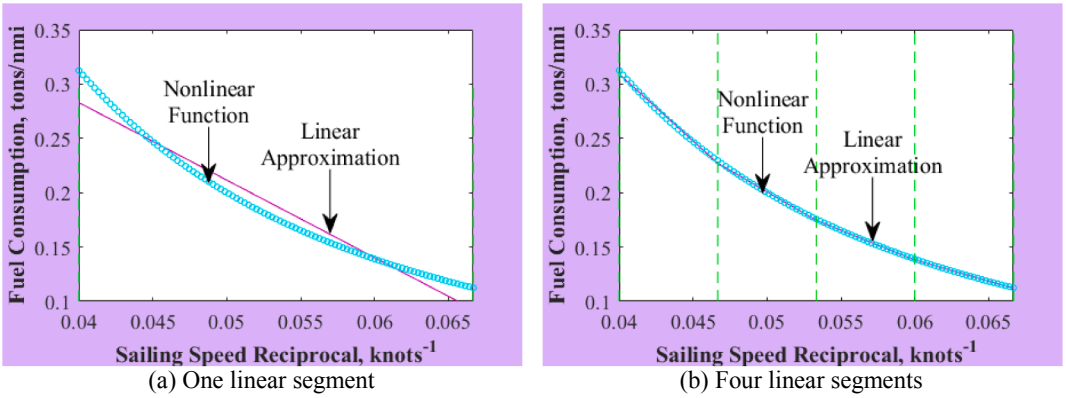

(a) One linear segment (b) Four linear segments

Fig. 4. Fuel consumption linear approximations.

$$Bn_{vs} \cdot \boldsymbol{g}_{rps} \le \boldsymbol{y}_{rp} \forall r \in R, p \in P_r, v \in V, s \in S_v \tag{30}$$

$$\boldsymbol{y}_{rp} \le Ed_{vs} + M_2 \cdot (1 - \boldsymbol{g}_{rps}) \forall r \in R, p \in P_r, v \in V, s \in S_v \tag{31}$$

$$\boldsymbol{RF}_{rpvs} \ge (Sl_{vs} \cdot \boldsymbol{y}_{rp} + In_{vs}) \cdot \left(\frac{\boldsymbol{QC}^{sea}_{rpv} \cdot AWC + LWT_v}{TWC_v + LWT_v}\right)^{\frac{2}{3}} - M_2 \cdot (1 - \boldsymbol{g}_{rps}) \forall r \in R, p \in P_r, v \in V, s \in S_v \tag{32}$$

The fourth group of constraints [i.e., constraints (33)-(40)] computes important time components that are used for tactical liner shipping decisions. In particular, constraints (33) compute the port handling time for each port under a given liner shipping route. Constraints (34) estimate the sailing time of ships between two consecutive ports. Constraints (35) and (36) quantify the waiting time of ships for each port under a given liner shipping route. Constraints (37) determine the late arrival hours for each port. Constraints (38) estimate the ship departure time from each port under a given liner shipping route. Constraints (39) and (40) identify the ship arrival time at the following port for each liner shipping route.

$$\boldsymbol{\tau}^{hand}_{rpth} = \frac{\boldsymbol{QC}^{PORT}_{rp}}{ph_{rpth}} \forall r \in R, p \in P_r, t \in T_{rp}, h \in H_{rpt} \tag{33}$$

$$\boldsymbol{\tau}^{sail}_{rp} = l_{rp} \cdot \boldsymbol{y}_{rp} \forall r \in R, p \in P_r \tag{34}$$

$$\boldsymbol{\tau}^{wait}_{r(p+1)} \ge \sum_{t \in T_{rp}} \tau^{st}_{r(p+1)t} \cdot \boldsymbol{z}_{r(p+1)t} - \boldsymbol{\tau}^{dep}_{rp} - \boldsymbol{\tau}^{sail}_{rp} \forall r \in R, p \in P_r, p < n^2_r \tag{35}$$

$$\boldsymbol{\tau}^{wait}_{r(1)} \ge \sum_{t \in T_{rp}} \tau^{st}_{r(1)t} \cdot \boldsymbol{z}_{r(1)t} - \boldsymbol{\tau}^{dep}_{rp} - \boldsymbol{\tau}^{sail}_{rp} + 24 \cdot \boldsymbol{\phi}_r \cdot \boldsymbol{q}_r \forall r \in R, p \in P_r, p = n^2_r \tag{36}$$

$$\boldsymbol{\tau}^{late}_{rp} \ge \boldsymbol{\tau}^{arr}_{rp} - \sum_{t \in T_{rp}} \tau^{end}_{rpt} \cdot \boldsymbol{z}_{rpt} \forall r \in R, p \in P_r \tag{37}$$

$$\boldsymbol{\tau}^{dep}_{rp} = \boldsymbol{\tau}^{arr}_{rp} + \boldsymbol{\tau}^{wait}_{rp} + \sum_{t \in T_{rp}} \sum_{h \in H_{rpt}} \boldsymbol{\tau}^{hand}_{rpth} \cdot \boldsymbol{x}_{rpth} \forall r \in R, p \in P_r \tag{38}$$

$$\boldsymbol{\tau}^{arr}_{r(p+1)} = \boldsymbol{\tau}^{dep}_{rp} + \boldsymbol{\tau}^{sail}_{rp} \forall r \in R, p \in P_r, p < n^2_r \tag{39}$$

$$\boldsymbol{\tau}^{arr}_{r(1)} = \boldsymbol{\tau}^{dep}_{rp} + \boldsymbol{\tau}^{sail}_{rp} - 24 \cdot \boldsymbol{\phi}_r \cdot \boldsymbol{q}_r \forall r \in R, p \in P_r, p = n^2_r \tag{40}$$

The fifth group of constraints [i.e., constraints (41)-(48)] imposes some operational requirements regarding the frequency of port service as well as the deployment of available ships. More specifically, constraints (41) guarantee that the ships will maintain a particular frequency of port service for each liner shipping route based on a profit maximization objective function. Constraints (42) limit the frequency of port service to a certain maximum value for each liner shipping route. Constraints (43) compute the total quantity of ships required for the deployment at each liner shipping route. Constraints (44) indicate that the ship types selected for a liner shipping route must be compatible to its ports of call. Constraints (45)-(48) indicate that the required quantity of the shipping line's own ships and chartered ships will not be over the available quantity of ships in the shipping line's fleet and the available quantity of ships to be chartered, respectively.

$$24 \cdot \boldsymbol{\phi}_r \cdot \boldsymbol{q}_r = \sum_{p \in P_r} \boldsymbol{\tau}^{sail}_{rp} + \sum_{p \in P_r} \sum_{t \in T_{rp}} \sum_{h \in H_{rpt}} \boldsymbol{\tau}^{hand}_{rpth} \cdot \boldsymbol{x}_{rpth} + \sum_{p \in P_r} \boldsymbol{\tau}^{wait}_{rp} \forall r \in R \tag{41}$$

$$\boldsymbol{\phi}_r \le \phi^{max} \forall r \in R \tag{42}$$

$$\boldsymbol{q}_r = \sum_{v \in V} (\boldsymbol{q}^{own}_{rv} + \boldsymbol{q}^{char}_{rv}) \forall r \in R \tag{43}$$

$$\boldsymbol{d}_{rv} \le d^0_{rv} \forall r \in R, v \in V \tag{44}$$

$$\boldsymbol{q}^{own}_{rv} \le q^{own-m}_v \cdot \boldsymbol{d}_{rv} \forall r \in R, v \in V \tag{45}$$

$$\sum_{r \in R} \boldsymbol{q}^{own}_{rv} \le q^{own-m}_v \forall v \in V \tag{46}$$

$$\boldsymbol{q}^{char}_{rv} \le q^{char-m}_v \cdot \boldsymbol{d}_{rv} \forall r \in R, v \in V \tag{47}$$

$$\sum_{r \in R} \boldsymbol{q}^{char}_{rv} \le q^{char-m}_v \forall v \in V \tag{48}$$

The sixth group of constraints determines the quantity of emissions to be generated at each voyage leg [i.e., constraints (49)] and for each port under a given liner shipping route [i.e., constraints (50)].

$$\boldsymbol{EP}^{SEA}_{rpv} = \sum_{s \in S_v} EF^{SEA} \cdot l_{rp} \cdot \boldsymbol{RF}_{rpvs} \forall r \in R, p \in P_r, v \in V \tag{49}$$

$$\boldsymbol{EP}^{PORT}_{rpv} = \boldsymbol{QC}^{PORT}_{rp} \cdot \sum_{t \in T_{rp}} \sum_{h \in H_{rpt}} (EF^{PORT}_{rphv} \cdot \boldsymbol{x}_{rpth}) \forall r \in R, p \in P_r, v \in V \tag{50}$$

The seventh (and the last) group of constraints [i.e., constraints (51)-(60)] computes different monetary components of the **TLP-HSF** objective function (19).

$$\boldsymbol{REV} = \sum_{r \in R} \sum_{p \in P_r} \sum_{v \in V} c^{rev}_{rp} \cdot \boldsymbol{QC}^{PORT}_{rp} \cdot (\boldsymbol{q}^{own}_{rv} + \boldsymbol{q}^{char}_{rv}) \tag{51}$$

$$\boldsymbol{SOC} = \sum_{r \in R} \sum_{v \in V} c^{oper}_v \cdot \boldsymbol{q}^{own}_{rv} \cdot \boldsymbol{\phi}_r \cdot (\boldsymbol{q}^{own}_{rv} + \boldsymbol{q}^{char}_{rv}) \tag{52}$$

$$\boldsymbol{SCC} = \sum_{r \in R} \sum_{v \in V} c^{char}_v \cdot \boldsymbol{q}^{char}_{rv} \cdot \boldsymbol{\phi}_r \cdot (\boldsymbol{q}^{own}_{rv} + \boldsymbol{q}^{char}_{rv}) \tag{53}$$

$$\boldsymbol{PHC} = \sum_{r \in R} \sum_{p \in P_r} \sum_{t \in T_{rp}} \sum_{h \in H_{rpt}} \sum_{v \in V} c^{hand}_{rpthv} \cdot \boldsymbol{QC}^{PORT}_{rp} \cdot \boldsymbol{x}_{rpth} \cdot (\boldsymbol{q}^{own}_{rv} + \boldsymbol{q}^{char}_{rv}) \tag{54}$$

$$\boldsymbol{LAC} = \sum_{r \in R} \sum_{p \in P_r} \sum_{v \in V} c^{late}_{rp} \cdot \boldsymbol{\tau}^{late}_{rp} \cdot (\boldsymbol{q}^{own}_{rv} + \boldsymbol{q}^{char}_{rv}) \tag{55}$$

$$\boldsymbol{FCC} = c^{fuel} \cdot \sum_{r \in R} \sum_{p \in P_r} \sum_{v \in V} \sum_{s \in S_v} l_{rp} \cdot \boldsymbol{RF}_{rpvs} \cdot (\boldsymbol{q}^{own}_{rv} + \boldsymbol{q}^{char}_{rv}) \tag{56}$$

$$\boldsymbol{CIC}^{SEA} = c^{inv} \cdot \sum_{r \in R} \sum_{p \in P_r} \sum_{v \in V} \boldsymbol{QC}^{SEA}_{rpv} \cdot \boldsymbol{\tau}^{sail}_{rp} \cdot (\boldsymbol{q}^{own}_{rv} + \boldsymbol{q}^{char}_{rv}) \tag{57}$$

$$\begin{aligned} \boldsymbol{CIC}^{PORT} = {} & c^{inv} \cdot \sum_{r \in R} \sum_{p \in P_r} \sum_{v \in V} \boldsymbol{QC}^{SEA}_{rpv} \cdot \boldsymbol{\tau}^{wait}_{rp} \cdot (\boldsymbol{q}^{own}_{rv} \\ & + \boldsymbol{q}^{char}_{rv}) + c^{inv} \cdot \sum_{r \in R} \sum_{p \in P_r} \sum_{t \in T_{rp}} \sum_{h \in H_{rpt}} \sum_{v \in V} \left(\boldsymbol{QC}^{SEA}_{rpv} \right. \\ & \left. - \boldsymbol{QC}^{PORT}_{rp}\right) \cdot \boldsymbol{\tau}^{hand}_{rpth} \cdot \boldsymbol{x}_{rpth} \cdot (\boldsymbol{q}^{own}_{rv} + \boldsymbol{q}^{char}_{rv}) \end{aligned} \tag{58}$$

$$\boldsymbol{EC}^{SEA} = c^{emis} \cdot \sum_{r \in R} \sum_{p \in P_r} \sum_{v \in V} \boldsymbol{EP}^{SEA}_{rpv} \cdot (\boldsymbol{q}^{own}_{rv} + \boldsymbol{q}^{char}_{rv}) \tag{59}$$

$$\boldsymbol{EC}^{PORT} = c^{emis} \cdot \sum_{r \in R} \sum_{p \in P_r} \sum_{v \in V} \boldsymbol{EP}^{PORT}_{rpv} \cdot (\boldsymbol{q}^{own}_{rv} + \boldsymbol{q}^{char}_{rv}) \tag{60}$$

4. Solution approach

Pasha et al. [41] presented an optimization model (**HOMTLP**), which addressed all the major tactical liner shipping decisions. However, the model assigned a homogeneous fleet of ships to each liner shipping route. Still, an exact optimization method (i.e., BARON) required extensive CPU times for the model in case of large-size problem instances. The **TLP-HSF** model developed herein is mathematically more complex than the aforementioned **HOMTLP** model, since it allows assigning a heterogeneous fleet of ships to a given liner shipping route. Thus, for the **TLP-HSF** model, tackling a number of liner shipping routes

altogether with an exact optimization method for mixed-integer nonlinear programming models (e.g., BARON) may not be pragmatic. The exact optimization method may not even provide any feasible solution within a reasonable amount of time for large-size instances of the problem. Hence, this study developed a heuristic algorithm, named the Recursive Route Decomposition Heuristic (RRDH), which can provide tactical-level planning decisions for the **TLP-HSF** model within a reasonable amount of time for realistic-size liner shipping routes.

RRDH is a decomposition-based heuristic. Decomposition-based methods have been widely used in different settings to solve complex decision problems [47–49]. The proposed RRDH sorts liner shipping routes and combines them into groups, considering the average unit freight rate and route type (e.g., service region, geographical characteristics) as sorting criteria. Each group of liner shipping routes is then tackled separately with an exact optimization method (e.g., BARON). For the purpose of grouping liner shipping routes, the average unit freight rate of liner shipping routes is employed as the primary sorting criterion, since RRDH intends to offer more choices of ship types for the liner shipping routes with higher freight rates (e.g., all the ships are available for the liner shipping routes with the highest freight rates, so a greater total turnaround profit could be obtained). Furthermore, the route type is used as the secondary sorting criterion, as greater convenience and ease of operations planning can be offered when the liner shipping routes with the same geographical characteristics or other features are grouped together (e.g., Asia-Europe routes vs. Trans-Pacific routes vs. Trans-Atlantic routes). As indicated earlier, many shipping lines tend to deploy heterogeneous fleets of ships for the Asia-Europe routes, where mega-ships are allocated to serve ports along with smaller ships [7]. In the meantime, heterogeneous fleets of ships could be observed at different Trans-Pacific routes and Trans-Atlantic routes as well. The main steps of the RRDH heuristic are highlighted in Algorithm 1.

Along with the notations that have been presented so far, additional notations are used in the RRDH pseudocode, including the following: (1) *Data* – input data for the **TLP-HSF** optimization model; (2) $\overline{c_r^{rev}}, r \in R$ – average unit freight rate that can be generated for liner shipping route r over the corresponding ports of call; (3) δ – decomposition parameter for RRDH (i.e., the maximum number of liner shipping routes that can be considered at a time throughout optimization); (4) $\overline{q_v^{own}}, v \in V$ – updated quantity of the shipping line's own ships of type v available; and (5) $\overline{q_v^{char}}, v \in V$ – updated quantity of ships of type v available for chartering. The main steps of RRDH are as follows. In step 0, the data structures are generated to store the tactical-level planning decisions (*TLPD*), as well as the average unit freight rate that can be generated for liner shipping route r over the corresponding ports of call ($\overline{c^{rev}}$), the updated quantity of the shipping line's own ships by ship type ($\overline{q^{own}}$), and the updated quantity of ships available for chartering by ship type ($\overline{q^{char}}$). In steps 1–5, the average unit freight rate ($\overline{c^{rev}}$) is calculated for each of the liner shipping routes.

Algorithm 1. Recursive Route Decomposition Heuristic (RRDH)

RRDH$(Data, R, V, q^{own-m}, q^{char-m}, c^{rev}, \delta)$
in: *Data* - input data for **TLP-HSF**; $R = \{1, \cdots, n^1\}$ - set of liner shipping routes; $V = \{1, \cdots, n^3\}$ - set of available ship types; q^{own-m} - available quantity of the shipping line's own ships by ship type; q^{char-m} - quantity of ships available for chartering by ship type; c^{rev} - unit freight rate by port and route; δ - decomposition parameter
out: *TLPD* - tactical-level planning decisions
0: $TLPD \leftarrow \emptyset$; $\left|\overline{c^{rev}}\right| \leftarrow n^1$; $\overline{q^{own}} \leftarrow q^{own-m}$; $\overline{q^{char}} \leftarrow q^{char-m}$ ◁ Initialization
1: $r \leftarrow 1$
2: **for** $r \in R$ **do**
3: $\overline{c_r^{rev}} \leftarrow$ ***Average***$_p(c_{rp}^{rev})$ ◁ Estimate the average unit freight rate for liner shipping route r
4: $r \leftarrow r + 1$
5: **end for**
6: $R \leftarrow$ ***Group***$(R, \overline{c^{rev}}, Data, \delta)$ ◁ Group the considered liner shipping routes
7: **while** $R \neq \emptyset$ **do**
8: $R^0 \leftarrow$ ***GroupSelect***(R) ◁ Select the next group of liner shipping routes for optimization

(*continued on next column*)

(*continued*)

9: $\left[TLPD, q_{rv}^{own}, q_{rv}^{char}\right] \leftarrow$ ***TLP-HSF***$(Data, R^0, \overline{q_v^{own}}, \overline{q_v^{char}})$ ◁ Solve the sub-problem
10: $R \leftarrow R - R^0$ ◁ Update the set of liner shipping routes
11: **for** $v \in V$ **do**
12: $\overline{q_v^{own}} \leftarrow \overline{q_v^{own}} - \sum_{r \in R} q_{rv}^{own}$ ◁ Update the quantity of own ships available
13: $\overline{q_v^{char}} \leftarrow \overline{q_v^{char}} - \sum_{r \in R} q_{rv}^{char}$ ◁ Update the quantity of ships available for chartering
14: **end for**
15: **end while**
16: **return***TLPD*

In step 6, the liner shipping routes are sorted into groups. The considered liner shipping routes are sorted based on the average unit freight rate as the primary sorting criterion and then based on the route type (e.g., service region, geographical characteristics) as the secondary sorting criterion, taking into account the RRDH decomposition parameter (δ). Let's consider a hypothetical scenario with the following routes:

- Trans-Pacific 1 ($\overline{c_r^{rev}} = 2,800$ USD per TEU)
- Trans-Pacific 2 ($\overline{c_r^{rev}} = 3,200$ USD per TEU)
- Asia-Europe 1 ($\overline{c_r^{rev}} = 5,000$ USD per TEU)
- Asia-Europe 2 ($\overline{c_r^{rev}} = 5,600$ USD per TEU)
- Asia-Europe 3 ($\overline{c_r^{rev}} = 4,100$ USD per TEU)

If $\delta = 2$ routes (i.e., two liner shipping routes can be grouped at most), then RRDH will sort the available routes in the following groups:

- ***Group 1***: Asia-Europe 2 and Asia-Europe 1 (since they have the highest average freight rate per route of $[5,600 + 5,000]/2 = 5,300$ USD per TEU and serve the Asia-Europe trade).
- ***Group 2***: Asia-Europe 3 (since it has the second highest average freight rate per route of 4,100 USD per TEU).
- ***Group 3***: Trans-Pacific 2 and Trans-Pacific 1 (since they have the third highest average freight rate per route of $[3,200 + 2,800]/2 = 3,000$ USD per TEU and serve the Trans-Pacific trade).

In steps 7–15, the groups of liner shipping routes are tackled as sub-problems. Particularly, in step 8, a group of liner shipping routes is selected to be solved as a sub-problem (i.e., all the major tactical-level planning decisions will be optimized for the selected group of liner shipping routes by solving the **TLP-HSF** optimization model for these liner shipping routes). In step 9, the sub-problem is solved with an exact optimization method (BARON will be used in this study). In step 10, the set of liner shipping routes is updated, discarding the liner shipping routes that have been already optimized. In steps 11–14, the available quantity of the shipping line's own ships and the quantity of ships available for chartering are updated, subtracting the quantity of ships that have been assigned to the already-optimized liner shipping routes (both own and chartered). Steps 8–14 are repeated until all the major tactical-level planning decisions are optimized for all the considered liner shipping routes.

5. Numerical experiments

A series of numerical experiments were conducted using 10 liner shipping routes, served by the Orient Overseas Container Line (OOCL), to showcase the performance of the **TLP-HSF** optimization model and the RRDH algorithm [50]. The numerical experiments were executed on an Intel® Core™ i7-7700 K processor with a Windows 10 operating system and 32 GB of RAM. The GAMS (General Algebraic Modeling System) was used to call BARON (i.e., the exact optimization method used in this study) in each RRDH iteration. The maximum runtime of BARON was set to 2 hours, while the allowable optimality gap was set to 1%. The liner shipping routes used in this study are presented in Fig. 5 and Table 1, where the voyage leg lengths, in nautical miles, are denoted

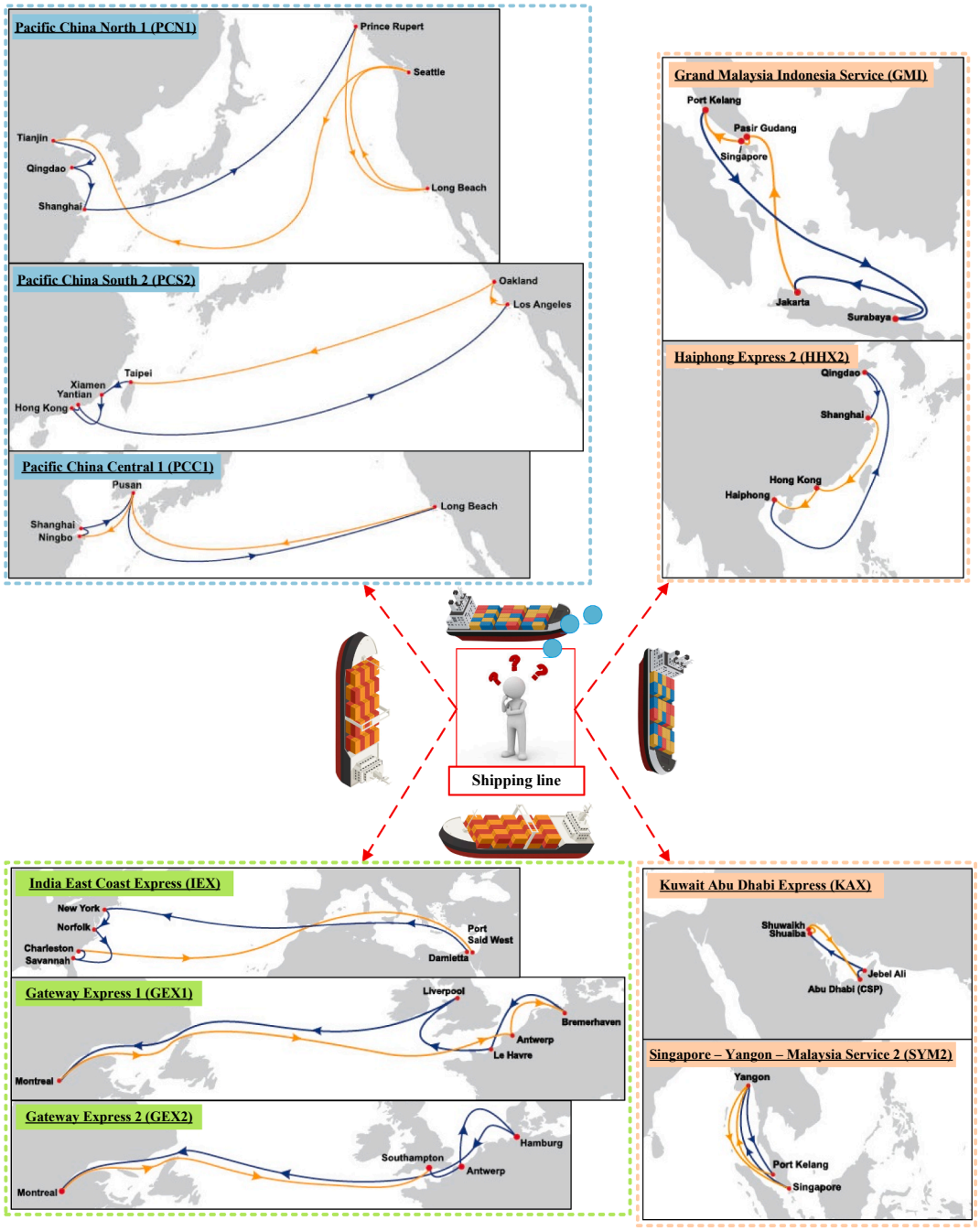

Fig. 5. Illustration of the liner shipping routes considered.

in parentheses [51]. Furthermore, the parameter values of the **TLP-HSF** model, which were used throughout this study, are shown in Table 2 [8,24,27,41,43,46,52,53].

5.1. Solution approach evaluation

The decomposition parameter of RRDH (δ), which denotes the maximum number of liner shipping routes that can be considered at a time throughout optimization, may directly impact the RRDH computational performance. Higher values of the decomposition parameter will likely improve the quality of solution, as more liner shipping routes will be considered for optimization at the same time. On the other hand, lower values of the decomposition parameter will likely reduce the CPU time. A set of randomly generated instances, consisting of multiple liner shipping routes, were used to determine the optimal value of the decomposition parameter and compare the RRDH computational performance against the exact optimization approach (i.e., BARON) that optimizes the tactical-level decisions for all the routes at the same time.

Results from the analysis that was conducted are presented in Table 3. The measure "objective gap" was used to determine the differences in the objective function values returned by BARON and RRDH. In particular, the objective gaps in Table 3 were estimated using the following equation: $\boldsymbol{Gap} = \left|\frac{Z^* - Z}{Z^*}\right|$, where Z^* is the objective function of BARON (when all the routes were solved together), and Z is the objective function returned by RRDH. Table 3 indicates that when the value of the decomposition parameter (δ) was 1 liner shipping route, the objective gaps ranged between −12.23% and 17.02%, with an average objective gap of 10.44%. Note that negative objective gaps indicate BARON being outperformed by RRDH. Negative objective gaps were

Table 1
Liner shipping routes considered.

Trans-Pacific Routes
Pacific China North 1 (PCN1): Tianjin (412) → Qingdao (399) → Shanghai (4,678) → Prince Rupert (1,443) → Long Beach (1,139) → Seattle (5,285) → Tianjin
Pacific China South 2 (PCS2): Taipei (198) → Xiamen (287) → Hong Kong (35) → Yantian (5,529) → Los Angeles (341) → Oakland (4,895) → Taipei
Pacific China Central 1 (PCC1): Ningbo (110) → Shanghai (492) → Pusan (5,230) → Long Beach (5,230) → Pusan (447) → Ningbo
Trans-Atlantic Routes
India East Coast Express (IEX): New York (287) → Norfolk (505) → Savannah (100) → Charleston (5,522) → Port Said West (33) → Damietta (4,414) → New York
Gateway Express 1 (GEX1): Montreal (3,295) → Antwerp (357) → Bremerhaven (452) → Le Havre (501) → Liverpool (3,001) → Montreal
Gateway Express 2 (GEX2): Montreal (3,063) → Southampton (257) → Antwerp (405) → Hamburg (3,412) → Montreal
Intra-Asia Routes
Grand Malaysia Indonesia Service (GMI): Port Kelang (1,236) → Surabaya (386) → Jakarta (554) → Pasir Gudang (28) → Singapore (230) → Port Kelang
Haiphong Express 2 (HHX2): Haiphong (1,900) → Qingdao (367) → Shanghai (955) → Hong Kong (1,548) → Haiphong
Kuwait Abu Dhabi Express (KAX): Shuaiba (26) → Shuwaikh (560) → Abu Dhabi (81) → Jebel Ali (536) → Shuaiba
Singapore – Yangon – Malaysia Service 2 (SYM2): Singapore (1,342) → Yangon (1,112) → Port Kelang (1,112) → Yangon (1,342) → Singapore

underscored in some instances where a total of five liner shipping routes (i.e., port rotations) were tackled. Moreover, BARON could not tackle any instances that involved six or more liner shipping routes. The computational performance of BARON is anticipated to worsen even further after increasing the quantity of liner shipping routes to be optimized due to the computational complexity of the **TLP-HSF** optimization model. Such a finding justifies the need for developing heuristic methods (like RRDH that was proposed herein). RRDH was able to solve the considered problem instances within a reasonable amount of time. In particular, when the value of δ was 1, there were significant savings in CPU time, as the average CPU time was 8.1 seconds, as compared to the average CPU time of 5,019.0 seconds required by BARON.

When the value of δ was 2, the objective gaps ranged between −20.61% and 4.55%, with an average objective gap of 0.03%. Hence, it can be concluded that there were significant differences between the objective gaps for $\delta = 2$ and the objective gaps for $\delta = 1$. As originally expected, RRDH returned superior solutions when the value of the decomposition parameter was 2 liner shipping routes (i.e., $\delta = 2$). In the instances where BARON was able to terminate before reaching the maximum time limit of 2 hours (e.g., instances #1, #2, #3, #4, #8), RRDH still produced near-optimal solutions with $\delta = 2$. The CPU times for RRDH with $\delta = 2$ were reasonable as well (average = 228.9 seconds). Note that no CPU time savings were found when the value of the decomposition parameter was 3 liner shipping routes or higher. Hence, the RRDH heuristic with a decomposition parameter of 2 liner shipping routes (i.e., $\delta = 2$) will be further used throughout the numerical experiments.

5.2. Impact of integrated decision making

In addition to the capability of assigning a heterogeneous fleet of ships to every liner shipping route, the **TLP-HSF** model captures all four of the major tactical liner shipping decisions. Thus, the decisions, provided by this integrated methodology, are optimal for each of the following problems: (i) determination of service frequency; (ii) ship fleet deployment; (iii) optimization of ship sailing speed; and (iv) design of ship schedules. If the decisions for one or more of the aforementioned decision problems are not provided by a model that involves tactical liner shipping decisions, then, significant losses of the total turnaround profit might occur. In order to support this statement, an additional analysis was conducted where the complexity of the **TLP-HSF** model was

Table 2
Parameter values used.

Notation	Denotation	Value
$n^3 \in \mathbb{N}$	quantity of ship types that are available (ship types)	3
$n^4_{rp} \in \mathbb{N} \forall r \in R, p \in P_r$	quantity of TWs that are available at port p of route r (TWs)	2
$n^5_{rpt} \in \mathbb{N} \forall r \in R, p \in P_r, t \in T_{rp}$	quantity of port HRs that are available at port p of route r during TW t	2
$\phi^{max} \in \mathbb{N}$	upper bound on frequency of port service (days)	14
$q^{own-m}_v \in \mathbb{N} \forall v \in V$	available quantity of ships of type v in the shipping line's own fleet (ships)	$U[2; 10]$*
$q^{char-m}_v \in \mathbb{N} \forall v \in V$	available quantity of chartered ships of type v (ships)	$U[2; 10]$
$d^0_{rv} \in \mathbb{B} \forall r \in R, v \in V$	=1 if type v ships can be deployed for route r (=0 otherwise)	$U[0; 1]$
$\vartheta^{max} \in \mathbb{R}^+$	maximum ship sailing speed (knots)	25
$\vartheta^{min} \in \mathbb{R}^+$	minimum ship sailing speed (knots)	15
$\alpha^{dem}_{rp} \in \mathbb{R}^+ \forall r \in R, p \in P_r$	coefficient that describes sensitivity of container demand to ship sailing speed reciprocal at port p of route r	$U[300; 1,600]$
$\beta^{dem}_{rp} \in \mathbb{R}^+ \forall r \in R, p \in P_r$	coefficient that describes sensitivity of container demand to ship sailing speed reciprocal at port p of route r	$U[2,500; 3,000]$
$Import_{rp} \in \mathbb{R}^+ \forall r \in R, p \in P_r$	proportion of import containers at port p of route r (%)	$U[45; 55]$
$QC^{SEA-0}_{rv} \in \mathbb{N} \forall r \in R, v \in V$	total amount of containers on a type v ship before the ship is docked at the first port for route r (TEUs)	$[6,000; 6,600]$
$ph_{rpth} \in \mathbb{R}^+ \forall r \in R, p \in P_r, t \in T_{rp}, h \in H_{rpt}$	handling productivity for HR h during TW t at port p of route r (TEUs per hour)	$U[50; 100]$
$AWC \in \mathbb{R}^+$	average cargo weight within a typical 20-ft container (tons)	11
$LWT_v \in \mathbb{R}^+ \forall v \in V$	empty weight of a ship of type v (tons)	$[46,000; 50,000]$
$TWC_v \in \mathbb{R}^+ \forall v \in V$	total carrying capacity of a ship of type v (tons)	$[138,000; 150,000]$
$\left[\tau^{end}_{rpt} - \tau^{st}_{rpt}\right] \in \mathbb{R}^+ \forall r \in R, p \in P_r, t \in T_{rp}$	arrival TW duration (hours)	$U[12; 48]$
$EF^{SEA} \in \mathbb{R}^+$	emission factor to be used in sea (tons of emissions per ton of fuel)	3.082**
$EF^{PORT}_{rphv} \in \mathbb{R}^+ \forall r \in R, p \in P_r, h \in H_{rpt}, v \in V$	emission factor to be used at port p of route r for HR h for ship type v (tons of emissions per TEU)	0.01729 for $h = 180$**
$c^{oper}_v \in \mathbb{R}^+ \forall v \in V$	unit cost of ship operating for ship type v (USD per day)	$[35,000; 43,000]$
$c^{char}_v \in \mathbb{R}^+ \forall v \in V$	unit cost of ship chartering for ship type v (USD per day)	$[53,000; 65,000]$
$c^{hand}_{rpthv} \in \mathbb{R}^+ \forall r \in R, p \in P_r, t \in T_{rp}, h \in H_{rpt}, v \in V$	unit cost of container handling at ports for ship type v at port p of route r during TW t for HR h (USD per TEU)	$U[200; 500]$
$c^{late}_{rp} \in \mathbb{R}^+ \forall r \in R, p \in P_r$	unit cost of late arrivals for port p of route r (USD per hour)	$U[5,000; 8,000]$
$c^{fuel} \in \mathbb{R}^+$	unit cost of fuel (USD per ton)	200
$c^{inv} \in \mathbb{R}^+$	unit cost of inventory (USD per TEU per hour)	0.25
$c^{emis} \in \mathbb{R}^+$	unit cost of emissions (USD per ton)	32**
$c^{rev}_{rp} \in \mathbb{R}^+ \forall r \in R, p \in P_r$	unit freight rate for delivery of cargo to port p of route r (USD	$U[5,200; 5,900]$

(*continued on next page*)

Table 2 (*continued*)

Notation	Denotation	Value
	per TEU)	
$M_1, M_2 \in \mathbb{R}^+$	sufficiently large positive numbers	[100,000,000; 100]

Notes: *U denotes a uniform distribution of pseudorandom numbers that have upper and lower bounds in square brackets; **Emissions of CO_2 were considered in this study with $EF^{SEA} = 3.082$ tons of CO_2 per ton of fuel, $EF^{PORT}_{rphv} = 0.01729$ for $h = 180$, and $c^{emis} = 32$ USD per ton [43,46].

reduced to formulate a less complicated model (will be referred to as **TLP-HSFR**), which did not determine service frequencies for liner shipping routes (i.e., ϕ_r was reduced to a parameter) and did not deploy ships to liner shipping routes (i.e., q^{own}_{rv} and q^{char}_{rv} were reduced to parameters). The **TLP-HSFR** model considered fixed weekly service frequency (i.e., $\phi_r = 7 \forall r \in R$), and the ship fleet deployment decisions were predetermined as well (i.e., ship types were assigned randomly to the considered routes). The other tactical-level decisions, including optimization of ship sailing speed and design of ship schedules, were still captured by the **TLP-HSFR** model.

The performances of the **TLP-HSF** model and the **TLP-HSFR** model were then compared using a large-size problem instance, generated with routes GMI, PCS2, GEX1, PCC1, HHX2, and KAX. Moreover, 10 scenarios were generated by altering the unit cost of ship operating from 8,000–10,000 USD per day in the first scenario to 80,000–100,000 USD per day in the last scenario, with increments of 8,000–10,000 USD per day. Both of the models were then solved with the RRDH algorithm for the aforementioned scenarios. Apart from the values of the unit cost of ship operating, the other parameter values were used from Table 2.

The values of objective function and CPU time for the **TLP-HSF** model and the **TLP-HSFR** model with fixed service frequency and fixed ship fleet deployment decisions are presented in Table 4. As it can be seen, the values of objective function (i.e., total turnaround profit values) were lower for the **TLP-HSFR** model for all of the tested scenarios. In particular, the **TLP-HSFR** objective function values were 22.94% lower on average when comparing to the **TLP-HSF** model. Since the **TLP-HSFR** model has less variables (the service frequency decisions and the ship fleet deployment decisions are fixed), its CPU time was lower when comparing to the CPU time of the **TLP-HSF** model. However, the average CPU time required to solve the **TLP-HSF** model comprised 592 seconds. Such a CPU time can be considered as acceptable from the perspective of practitioners (i.e., a shipping line should be able to conduct tactical-level planning for its liner shipping routes in a timely manner). The analysis that was conducted in this section of the manuscript highlights the importance of integrated decision making and shows that shipping lines may incur substantial losses of the total profit when addressing tactical-level decisions separately.

5.3. Managerial insights

This section presents some managerial insights, gained from the proposed methodology, based on a detailed solution analysis. The purpose of the analysis, conducted in this section, was to identify the differences in tactical-level decisions among the considered liner shipping routes based on the average freight rates for these liner shipping routes, as the average freight rates can be viewed as the major determinants of the total profit that could be potentially generated by a given shipping line. In order to perform the analysis, a large-size problem instance was used with liner shipping routes GEX1, IEX, PCC1, SYM2, PCS2, and PCN1 that had the average freight rates of 5,361.80 USD per TEU, 5,454.83 USD per TEU, 5,570.20 USD per TEU, 5,659.75 USD per TEU,

Table 3
RRDH heuristic evaluation.

Instance	Routes (Number of Ports of Call)	All Routes Solved Together by BARON		Routes Solved One by One (i.e., RRDH with $\delta = 1$)			Two Routes Solved Together (i.e., RRDH with $\delta = 2$)		
		Objective Function (USD)	CPU Time (sec)	Objective Function (USD)	CPU Time (sec)	Objective Gap (%)	Objective Function (USD)	CPU Time (sec)	Objective Gap (%)
1	GMI (5), PCS2 (6)	447,034,574	149.8	397,130,157	3.5	11.16	447,034,574	149.8	0.00
2	GEX1 (5), KAX (4)	336,130,549	244.9	289,516,474	1.6	13.87	336,130,549	244.9	0.00
3	HHX2 (4), PCC1 (5)	413,071,804	168.9	352,208,558	4.9	14.73	413,071,804	168.9	0.00
4	GEX1 (5), GEX2 (4)	335,640,164	72.7	284,061,230	1.7	15.37	335,640,164	72.7	0.00
5	GEX1 (5), IEX (6), PCN1 (6)	622,324,082	7,200.0	584,207,630	5.6	6.12	596,048,253	90.9	4.22
6	HHX2 (4), IEX (6), PCC1 (5)	639,501,298	7,200.0	575,620,996	7.6	9.99	636,484,242	171.6	0.47
7	GEX1 (5), HHX2 (4), PCC1 (5)	594,477,098	7,200.0	520,053,067	6.0	12.52	580,916,313	170.0	2.28
8	HHX2 (4), KAX (4), SYM2 (4)	489,634,360	467.8	430,955,028	8.5	11.98	467,363,534	297.4	4.55
9	GMI (5), HHX2 (4), IEX (6), PCS2 (6)	868,908,039	7,200.0	759,348,481	6.7	12.61	851,031,756	235.0	2.06
10	GMI (5), HHX2 (4), PCC1 (5), PCS2 (6)	867,829,599	7,200.0	749,338,715	8.5	13.65	860,106,378	318.7	0.89
11	HHX2 (4), PCC1 (5), PCN1 (6), SYM2 (4)	800,436,255	7,200.0	715,636,418	14.3	10.59	791,117,963	265.6	1.16
12	GEX1 (5), HHX2 (4), PCC1 (5), KAX (4)	773,381,182	7,200.0	641,725,032	6.5	17.02	749,202,353	413.8	3.13
13	GEX1 (5), GMI (5), HHX2 (4), PCC1 (5), PCS2 (6)	1,051,497,398	7,200.0	917,183,224	9.6	12.77	1,027,950,887	319.8	2.24
14	GMI (5), HHX2 (4), IEX (6), PCC1 (5), PCS2 (6)	1,087,256,280	7,200.0	972,751,153	11.2	10.53	1,083,518,816	321.4	0.34
15	GMI (5), HHX2 (4), IEX (6), PCC1 (5), SYM2 (4)	972,937,124	7,200.0	911,638,360	17.6	6.30	975,530,929	211.9	−0.27
16	GEX1 (5), GMI (5), HHX2 (4), PCC1 (5), SYM2 (4)	762,757,378	7,200.0	856,070,431	16.0	−12.23	919,963,000	210.3	−20.61
Average:		691,426,074	5,019.0	622,340,310	8.1	10.44	691,944,470	228.9	0.03

Table 4
Objective functions and CPU times of the **TLP-HSF** model and the **TLP-HSFR** model with fixed service frequency and fixed ship fleet deployment decisions.

Scenario	Unit Cost of Ship Operating (USD per day)	Service Frequency and Ship Fleet Deployment Decisions			
		Objective Function (USD)		CPU Time (sec)	
		Variable	Fixed	Variable	Fixed
1	[8,000; 10,000]	1,206,474,487	945,188,645	633.3	65.8
2	[16,000; 20,000]	1,205,020,391	939,140,645	252.3	25.0
3	[24,000; 30,000]	1,201,349,166	933,092,645	374.2	84.9
4	[32,000; 40,000]	1,185,077,103	927,044,645	882.3	63.6
5	[40,000; 50,000]	1,196,773,011	920,996,645	564.8	69.9
6	[48,000; 60,000]	1,192,261,780	914,948,645	475.8	60.2
7	[56,000; 70,000]	1,178,164,301	908,900,645	650.5	56.5
8	[64,000; 80,000]	1,185,691,551	902,852,645	710.0	69.5
9	[72,000; 90,000]	1,181,413,113	896,804,645	650.9	69.7
10	[80,000; 100,000]	1,180,060,481	890,756,645	729.5	69.1
Average:		1,191,228,538	917,972,645	592.3	63.4

5,749.50 USD per TEU, and 5,834.17 USD per TEU, respectively. For this instance, all the parameter values were used from Table 2, and the **TLP-HSF** model was solved with the RRDH algorithm. The managerial insights were obtained from the solution returned by the RRDH algorithm for this large-size problem instance. Fig. 6 illustrates the sensitivity patterns of the average ship sailing speed, the average ship carrying capacity, the average handling productivity at ports, and the average frequency of service to the average freight rate.

It can be noticed that the average ship sailing speed was increased with the average freight rate. Therefore, the solution approach directed the ships to sail faster along the routes with higher average freight rates. This increase can be justified by the fact that the container demand in the **TLP-HSF** model is proportional to the ship sailing speed. When the ship sailing speed was increased, the container demand was also increased for the routes with higher average freight rates. Hence, more revenue was generated from such routes, and the total turnaround profit was generally higher. Furthermore, the average carrying capacity was increased with the average freight rate. Therefore, the solution approach allocated larger ships to the routes with higher average freight rates. This increase can be explicated by the fact that when the average freight rate was higher, the container demand increased due to increasing ship sailing speed, and the developed solution algorithm aimed to load the additional container demand to the ships with higher carrying capacity (so that a higher profit could be achieved). Hence, it can be concluded that shipping lines would be able to generate more profit from the deployment of mega-ships at the routes with higher freight rates, which is in accordance with practice.

Results from the conducted analysis also showed that the average handling productivity at ports was generally increased with the average freight rate. Therefore, the solution approach assigned handling rates that have higher handling productivities to the routes with higher average freight rates. Higher port handling productivities were required to prevent an increase in the total port handling time due to increasing container demand (as the container demand increased with the ship sailing speed). An increase of the total port handling time would further increase the total turnaround time of ships and necessitate more ships for deployment to maintain the target frequency of port service. The deployment of more ships is not desirable, as it would result in the total turnaround profit losses. The numerical experiments also showed that the ports were generally visited less frequently (i.e., the number of days between subsequent ship arrivals, which is the duration between subsequent port visits, was higher) for the routes with higher average freight rates. Therefore, the solution approach assigned longer duration between subsequent port visits for the routes with higher average freight rates. A longer duration between subsequent port visits was required to prevent an increase of the total cost of ship operating and the total cost of ship chartering for each route, as more frequent service of ports would necessitate the deployment of more ships (i.e., shipping line's own ships and/or chartered ships) that may further reduce the total turnaround profit of the shipping line.

As a part of the numerical experiments, a supplementary analysis

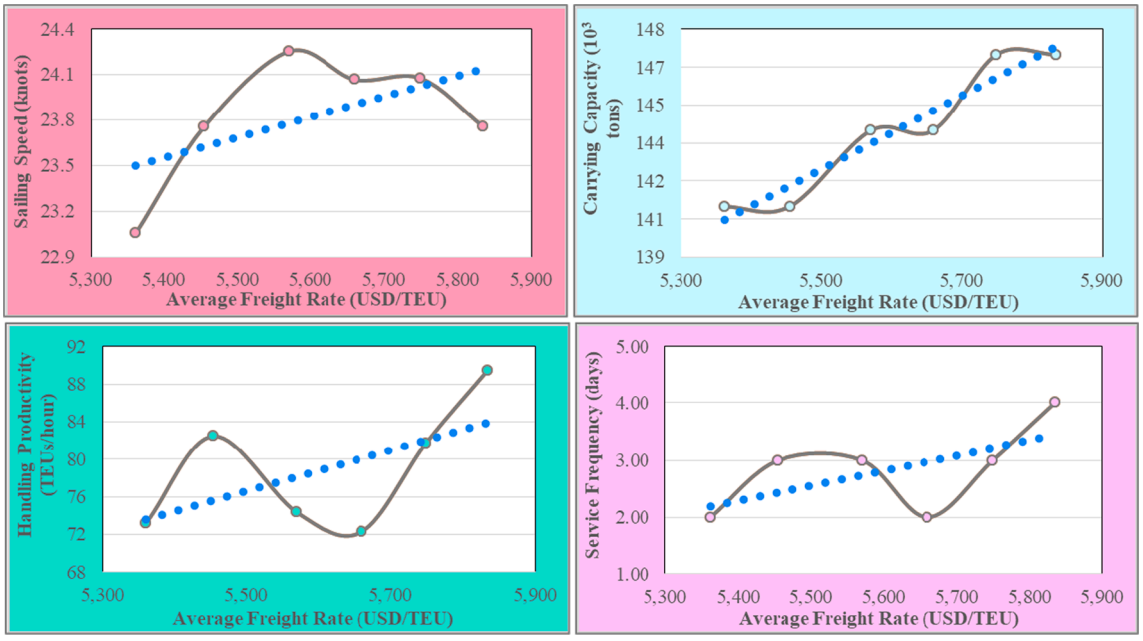

Fig. 6. Sensitivity patterns of the average ship sailing speed, the average ship carrying capacity, the average handling productivity at ports, and the average frequency of service to the average freight rate.

was performed to investigate the relationship between the total quantity of emissions generated at voyage legs in sea and the average freight rate for the considered routes. Emissions of carbon dioxide (CO_2) were modeled in this study. The CO_2 emission factor to be used in sea (EF^{SEA}) comprises 3.082 tons of CO_2 per ton of fuel, while the CO_2 emission factor to be used at ports due to handling of containers ($EF^{PORT}_{rphv}, r \in R, p \in P_r, h \in H_{rpt}, v \in V$) comprises 0.01729 tons of CO_2 per TEU for the baseline container handling productivity of 180 TEUs per hour [43,46] – see Table 2. It was found that the total quantity of emissions generated at voyage legs in sea was generally increased with the average freight rate (see Fig. 7). Therefore, the shipping line was mostly driven with the economic perspectives (i.e., maximize the total turnaround profit) rather than the environmental perspectives (i.e., minimize the total quantity of emissions generated in sea). Note that the patterns in the emissions due to container handling at ports were not investigated throughout the experiments as they were not significant when comparing to the quantity of emissions generated at voyage legs in sea (i.e., ≈8,000 tons of CO_2 were generated on average at ports for the considered routes vs. ≈72,000 tons of CO_2 were generated at voyage legs on average in sea for the considered routes).

A number of alternatives can be considered by the relevant stakeholders to alleviate the negative consequences from liner shipping on the environment. First, imposing a higher unit cost of emissions (c^{emis} – USD per ton) or "emission tax" is likely to reduce the ship sailing speed, as the shipping line would aim to prevent an excessive total cost of emissions due to hauling of ships in sea (since the emission cost in sea directly impacts the total turnaround profit of the shipping line). Second, appropriate environmental regulations could be introduced for the ships sailing in specific geographical locations (e.g., introduction of "emission control areas", introduction of new requirements for ship engines). Third, a number of alternative methods could be applied to decrease the quantity of emissions from ships (e.g., renewable energy sources, alternative fuels, hydrodynamic measures, ship design measures, ship machinery measures, improved energy efficiency, qualifications of ship crew, and others).

Another interesting finding that was revealed during the numerical experiments consists in the fact that the total turnaround profit does not necessarily increase with the average freight rate (see Fig. 8). Such a pattern can be justified by the differences in the representative route attributes (e.g., length of voyage legs, quantity of ports to be served). For example, the total turnaround profit values for the IEX and SYM2 routes were found to be 223.4 million USD and 170.5 million USD, respectively, despite the fact that the average IEX freight rate comprises 5,454.83 USD per TEU, while the average SYM2 freight rate comprises 5,659.75 USD per TEU. A lower total turnaround profit was recorded for the SYM2 route when comparing to the IEX route, since the IEX route has 6 ports, while the SYM2 route has 4 ports (i.e., more profit was generated for the IEX route due to service of additional ports of call). The differences in the representative route attributes caused some fluctuations in the patterns for some other variables of the **TLP-HSF** model as well (see Fig. 6 and Fig. 7). For instance, the conducted analysis showed

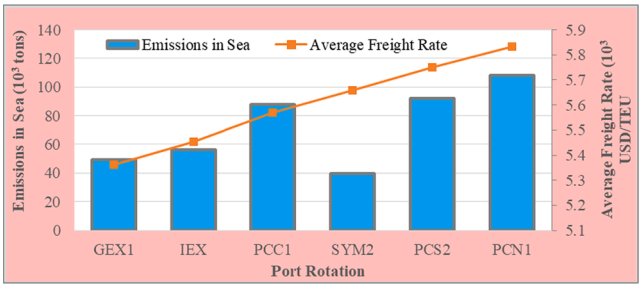

Fig. 7. Relationship between the total quantity of emissions generated in sea and the average freight rate for the considered routes.

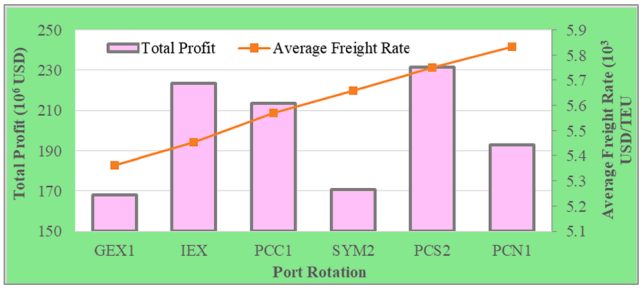

Fig. 8. Relationship between the total turnaround profit and the average freight rate for the considered routes.

that the ports were generally visited less frequently for the routes with higher average freight rates. However, the ports of the SYM2 route were visited more frequently than the ports of the IEX and PCC1 routes, despite the fact that the SYM2 route has higher average freight rate when comparing to the IEX and PCC1 routes. The latter finding can be explained by fewer ports of call for the SYM2 route (i.e., the total cost of ship operating and the total cost of ship chartering for the SYM2 route did not increase substantially with more frequent port service as fewer ports had to be served).

Considering the findings from the computational experiments performed, it can be concluded that the developed **TLP-HSF** optimization model and the proposed RRDH heuristic may serve as an effective decision support system to shipping lines when addressing the major tactical liner shipping decisions (i.e., determination of service frequency, ship fleet deployment, optimization of ship sailing speed, and design of ship schedules) for liner shipping routes that are served not only by homogenous ship fleets but also by heterogeneous ship fleets as well. Moreover, the developed **TLP-HSF** optimization model is expected to support environmental sustainability throughout liner shipping and minimize emissions of harmful substances.

6. Conclusions

The current trends in liner shipping show a continuous growth in ship size. More and more small ships are being replaced with large ships, which is leading to the deployment of heterogeneous ship fleets along different routes. Nonetheless, the existing mathematical models, which address the major tactical liner shipping decisions, typically assume the deployment of a homogeneous ship fleet along a given route. Taking into account the existing tendencies of liner shipping operations, this study presented a novel Integrated Optimization Model for Tactical-Level Planning Decisions in Liner Shipping with Heterogeneous Ship Fleet and Environmental Considerations (**TLP-HSF**) that addressed all the major tactical liner shipping decisions (i.e., determination of service frequency, ship fleet deployment, optimization of ship sailing speed, and design of ship schedules) and allowed the deployment of a heterogeneous ship fleet at each liner shipping route, considering emissions generated throughout liner shipping operations. The model's objective function was to maximize the total turnaround profit. The major costs in liner shipping, found in the literature, were incorporated in the **TLP-HSF** optimization model, which included: (1) the total cost of ship operating; (2) the total cost of ship chartering; (3) the total cost of container handling at ports; (4) the total cost of late arrivals; (5) the total cost of fuel consumption; (6) the total cost of inventory in sea as well as at ports; and (7) the total cost of emissions in sea as well as at ports.

Considering the computational complexity of the **TLP-HSF** optimization model, a decomposition-based heuristic algorithm, named the Recursive Route Decomposition Heuristic (RRDH), was developed to solve the model for large-size instances. The RRDH algorithm sorted routes into groups, considering the average unit freight rate and route type (e.g., service region, geographical characteristics). Each group of routes was then tackled separately with an exact optimization method (i.

e., BARON). Numerical experiments were conducted for a total of 10 real-world liner shipping routes served by OOCL. It was found that the proposed decomposition-based heuristic yielded good-quality solutions and required much lower computational time when comparing to the exact optimization method executed for all the considered routes at the same time. In order to illustrate the importance of integrated decision making, the performance of the **TLP-HSF** optimization model was compared with that of a less complicated model with fixed service frequency and fixed ship fleet deployment decisions. Results showed that the average total turnaround profit was 22.94% lower for the model with fixed service frequency and fixed ship fleet deployment decisions. Therefore, the **TLP-HSF** optimization model, which is an integrated decision-making model, could provide more profitable decisions for shipping lines.

A set of additional analyses were conducted to identify the differences in tactical-level decisions among the considered liner shipping routes based on the average freight rates for these liner shipping routes, as the average freight rates can be viewed as the major determinants of the total profit that could be potentially generated by a given shipping line. It was found that the average ship sailing speed, the average ship carrying capacity, and the average handling productivity at ports were generally increased with the average freight rate. However, the ports were generally visited less frequently (i.e., the number of days between subsequent ship arrivals, which is the duration between subsequent port visits, was higher) for the routes with higher average freight rates to prevent an increase of the total cost of ship operating and the total cost of ship chartering for each route. Moreover, the total quantity of emissions generated at voyage legs in sea was generally increased with the average freight rate. Hence, the shipping line was mostly driven with the economic perspectives (i.e., maximize the total turnaround profit) rather than the environmental perspectives (i.e., minimize the total quantity of emissions generated in sea). On the contrary, the quantity of emissions due to container handling at ports was found to be insignificant when comparing to the quantity of emissions generated in sea.

Considering the findings from the computational experiments performed, it can be concluded that the developed **TLP-HSF** optimization model and the proposed RRDH heuristic may serve as an effective decision support system to shipping lines when addressing the main tactical liner shipping decisions for liner shipping routes that are served not only by homogenous ship fleets but also by heterogeneous ship fleets as well. Moreover, the developed **TLP-HSF** optimization model is expected to support environmental sustainability throughout liner shipping and minimize emissions of harmful substances. This research can be extended further in several ways, including the following: (i) development of metaheuristic algorithms for the **TLP-HSF** optimization model; (ii) further analysis of container demand fluctuations due to different geo-political and economic factors; (iii) forecasting of freight rates for different liner shipping routes; (iv) consideration of different uncertainties that can occur throughout liner shipping operations, namely uncertainties in sailing times of ships, port times, sea weather conditions, shipment demand, etc.; (v) consideration of transshipment of cargoes at ports; (vi) modeling negotiations with alliance partners; and others.

Declaration of Competing Interest

The authors declare that they have no known competing financial interests or personal relationships that could have appeared to influence the work reported in this paper.

Acknowledgment

This research has been partially supported by the grant CMMI-1901109 of the National Science Foundation (United States). The opinions, conclusions, and findings, stated in this study, are those of the authors and do not necessarily represent the views of the National Science Foundation (United States).

Appendix. A. Nomenclature

Sets

$R = \{1, \cdots, n^1\}$	set of liner shipping routes considered (liner shipping routes)
$P_r = \{1, \cdots, n_r^2\}, r \in R$	set of ports for liner shipping route r (ports)
$V = \{1, \cdots, n^3\}$	set of ship types that are available (ship types)
$T_{rp} = \{1, \cdots, n_{rp}^4\}, r \in R, p \in P_r$	set of TWs that are available at port p for route r (TWs)
$H_{rpt} = \{1, \cdots, n_{rpt}^5\}, r \in R, p \in P_r, t \in T_{rp}$	set of port HRs that are available at port p for route r during TW t (HRs)
$S_v = \{1, \cdots, n_v^6\}, v \in V$	set of linear segments to be used in the piecewise function for consumption of fuel for type v ships (segments)

Decision variables

$\vartheta_{rp} \in \mathbb{R}^+ \forall r \in R, p \in P_r$	sailing speed of a ship at voyage leg p of route r (knots)
$\phi_r \in \mathbb{N} \forall r \in R$	frequency of port service for route r (days)
$q_{rv}^{own} \in \mathbb{N} \forall r \in R, v \in V$	quantity of ships of type v in the shipping line's own fleet assigned to route r (ships)
$q_{rv}^{char} \in \mathbb{N} \forall r \in R, v \in V$	quantity of chartered ships of type v assigned to route r (ships)
$d_{rv} \in \mathbb{B} \forall r \in R, v \in V$	=1 if ship type v is deployed for service of route r (=0 otherwise)
$z_{rpt} \in \mathbb{B} \forall r \in R, p \in P_r, t \in T_{rp}$	=1 if TW t is to be used at port p of route r (=0 otherwise)
$x_{rpth} \in \mathbb{B} \forall r \in R, p \in P_r, t \in T_{rp}, h \in H_{rpt}$	=1 if HR h is selected by the shipping line at port p of route r during TW t (=0 otherwise)
$g_{rps} \in \mathbb{B} \forall r \in R, p \in P_r, s \in S_v$	=1 if linear segment s is chosen for determination of fuel consumption at voyage leg p of route r (=0 otherwise)

Auxiliary variables

$q_r \in \mathbb{N} \forall r \in R$	total quantity of ships required for route r (ships)
$RF_{rpvs} \in \mathbb{R}^+ \forall r \in R, p \in P_r, v \in V, s \in S_v$	fuel consumption value under linear segment s for ship type v at voyage leg p of route r (tons per nmi)
$QC^{SEA}_{rpv} \in \mathbb{N} \forall r \in R, p \in P_r, v \in V$	amount of containers transported by a type v ship at voyage leg p of route r (TEUs)
$QC^{PORT}_{rp} \in \mathbb{N} \forall r \in R, p \in P_r$	amount of containers to be loaded/unloaded at port p of route r (TEUs)
$\tau^{sail}_{rp} \in \mathbb{R}^+ \forall r \in R, p \in P_r$	sailing time of a ship at voyage leg p of route r (hours)
$\tau^{arr}_{rp} \in \mathbb{R}^+ \forall r \in R, p \in P_r$	arrival time of a ship at port p of route r (hours)
$\tau^{wait}_{rp} \in \mathbb{R}^+ \forall r \in R, p \in P_r$	waiting time of a ship at port p of route r (hours)
$\tau^{late}_{rp} \in \mathbb{R}^+ \forall r \in R, p \in P_r$	late arrival time of a ship at port p of route r (hours)
$\tau^{hand}_{rpth} \in \mathbb{R}^+ \forall r \in R, p \in P_r, t \in T_{rp}, h \in H_{rpt}$	handling time of a ship at port p of route r during TW t for HR h (hours)
$\tau^{dep}_{rp} \in \mathbb{R}^+ \forall r \in R, p \in P_r$	departure time of a ship from port p of route r (hours)
$EP^{SEA}_{rpv} \in \mathbb{R}^+ \forall r \in R, p \in P_r, v \in V$	quantity of emissions generated by a type v ship at voyage leg p of route r (tons)
$EP^{PORT}_{rpv} \in \mathbb{R}^+ \forall r \in R, p \in P_r, v \in V$	quantity of emissions generated due to container handling for a type v ship at port p of route r (tons)
$REV \in \mathbb{R}^+$	total revenue (USD)
$SOC \in \mathbb{R}^+$	total cost of ship operating (USD)
$SCC \in \mathbb{R}^+$	total cost of ship chartering (USD)
$PHC \in \mathbb{R}^+$	total cost of container handling at ports (USD)
$LAC \in \mathbb{R}^+$	total cost of late arrivals (USD)
$FCC \in \mathbb{R}^+$	total cost of fuel consumption (USD)
$CIC^{SEA} \in \mathbb{R}^+$	total cost of inventory in sea (USD)
$CIC^{PORT} \in \mathbb{R}^+$	total cost of inventory at ports (USD)
$EC^{SEA} \in \mathbb{R}^+$	total cost of emissions in sea (USD)
$EC^{PORT} \in \mathbb{R}^+$	total cost of emissions at ports (USD)

Parameters

$n^1 \in \mathbb{N}$	quantity of liner shipping routes considered (liner shipping routes)
$n^2_r \in \mathbb{N} \forall r \in R$	quantity of ports for route r (ports)
$n^3 \in \mathbb{N}$	quantity of ship types that are available (ship types)
$n^4_{rp} \in \mathbb{N} \forall r \in R, p \in P_r$	quantity of TWs that are available at port p for route r (TWs)
$n^5_{rpt} \in \mathbb{N} \forall r \in R, p \in P_r, t \in T_{rp}$	quantity of port HRs that are available at port p for route r during TW t (HRs)
$n^6_v \in \mathbb{N} \forall v \in V$	quantity of linear segments in the piecewise function for consumption of fuel for type v ships (segments)
$l_{rp} \in \mathbb{R}^+ \forall r \in R, p \in P_r$	length of voyage leg p of route r (nmi)
$\vartheta^{max} \in \mathbb{N}$	upper bound on frequency of port service (days)
$q^{own-m}_v \in \mathbb{N} \forall v \in V$	available quantity of ships of type v in the shipping line's own fleet (ships)
$q^{char-m}_v \in \mathbb{N} \forall v \in V$	available quantity of chartered ships of type v (ships)
$d^0_{rv} \in \mathbb{B} \forall r \in R, v \in V$	=1 if type v ships can be deployed for service of route r (=0 otherwise)
$\vartheta^{max} \in \mathbb{R}^+$	maximum ship sailing speed (knots)
$\vartheta^{min} \in \mathbb{R}^+$	minimum ship sailing speed (knots)
$Sl_{vs} \in \mathbb{R}^+ \forall v \in V, s \in S_v$	slope for the function of fuel consumption for linear segment s of ship type v (ton per hour)
$In_{vs} \in \mathbb{R}^+ \forall v \in V, s \in S_v$	intercept for the function of fuel consumption for linear segment s of ship type v (tons per nmi)
$Bn_{vs} \in \mathbb{R}^+ \forall v \in V, s \in S_v$	reciprocal of ship sailing speed at the start of linear segment s for ship type v (knots^{-1})
$Ed_{vs} \in \mathbb{R}^+ \forall v \in V, s \in S_v$	reciprocal of ship sailing speed at the end of linear segment s for ship type v (knots^{-1})
$\alpha^{dem}_{rp}, \beta^{dem}_{rp} \in \mathbb{R}^+ \forall r \in R, p \in P_r$	coefficients that describe sensitivity of container demand to ship sailing speed reciprocal at port p of route r
$Import_{rp} \in \mathbb{R}^+ \forall r \in R, p \in P_r$	proportion of import containers at port p of route r (%)
$QC^{SEA-0}_{rv} \in \mathbb{N} \forall r \in R, v \in V$	total amount of containers on a type v ship before the ship is docked at the first port for route r (TEUs)
$ph_{rpth} \in \mathbb{R}^+ \forall r \in R, p \in P_r, t \in T_{rp}, h \in H_{rpt}$	handling productivity for HR h during TW t at port p of route r (TEUs per hour)
$AWC \in \mathbb{R}^+$	average cargo weight within a typical 20-ft container (tons)
$LWT_v \in \mathbb{R}^+ \forall v \in V$	empty weight of a ship of type v (tons)
$TWC_v \in \mathbb{R}^+ \forall v \in V$	total carrying capacity of a ship of type v (tons)
$\tau^{st}_{rpt} \in \mathbb{R}^+ \forall r \in R, p \in P_r, t \in T_{rp}$	TW t start at port p of route r (hours)
$\tau^{end}_{rpt} \in \mathbb{R}^+ \forall r \in R, p \in P_r, t \in T_{rp}$	TW t end at port p of route r (hours)
$EF^{SEA} \in \mathbb{R}^+$	emission factor to be used in sea (tons of emissions per ton of fuel)
$EF^{PORT}_{rphv} \in \mathbb{R}^+ \forall r \in R, p \in P_r, h \in H_{rpt}, v \in V$	emission factor to be used at port p of route r for HR h for ship type v (tons of emissions per TEU)
$c^{oper}_v \in \mathbb{R}^+ \forall v \in V$	unit cost of ship operating for ship type v (USD per day)
$c^{char}_v \in \mathbb{R}^+ \forall v \in V$	unit cost of ship chartering for ship type v (USD per day)
$c^{hand}_{rpthv} \in \mathbb{R}^+ \forall r \in R, p \in P_r, t \in T_{rp}, h \in H_{rpt}, v \in V$	unit cost of container handling at ports for ship type v at port p of route r during TW t for HR h (USD per TEU)
$c^{late}_{rp} \in \mathbb{R}^+ \forall r \in R, p \in P_r$	unit cost of late arrivals for port p of route r (USD per hour)
$c^{fuel} \in \mathbb{R}^+$	unit cost of fuel (USD per ton)
$c^{inv} \in \mathbb{R}^+$	unit cost of inventory (USD per TEU per hour)
$c^{emis} \in \mathbb{R}^+$	unit cost of emissions (USD per ton)
$c^{rev}_{rp} \in \mathbb{R}^+ \forall r \in R, p \in P_r$	unit freight rate for delivery of cargo to port p of route r (USD per TEU)
$M_1, M_2 \in \mathbb{R}^+$	sufficiently large positive numbers

References

[1] Q. Meng, S. Wang, H. Andersson, K. Thun, Containership routing and scheduling in liner shipping: overview and future research directions, Transport. Sci. 48 (2) (2014) 265–280.

[2] L. Zhen, S. Wang, G. Laporte, Y. Hu, Integrated planning of ship deployment, service schedule and container routing, Comput. Oper. Res. 104 (2019) 304–318.

[3] A. Prokopowicz, J. Berg-Andreassen, An evaluation of current trends in container shipping industry, very large container ships (VLCSs), and port capacities to accommodate TTIP increased trade, Transp. Res. Procedia 14 (2016) 2910–2919.

[4] The Maritime Executive, 2020. In down market, HMM takes delivery of world's biggest boxship. [online] https://www.maritime-executive.com/article/in-down-market-hmm-takes-delivery-of-world-s-biggest-boxship-at-geoje [Accessed 24 October 2020].

[5] M.A. Dulebenets, The vessel scheduling problem in a liner shipping route with heterogeneous fleet, Int. J. Civil Eng. 16 (1) (2018) 19–32.

[6] Journal of Commerce, 2014. Global ports grapple with congestion generated by larger ships and alliances. [online] https://www.joc.com/global-ports-grapple-congestion-generated-larger-ships-and-alliances_20140825.html [Accessed 24 October 2020].

[7] CMA CGM, 2020. Transport solutions from Asia to Europe. [online] https://www.cma-cgm.com/products-services/line-services/solution?ZoneFrom=ASIE&ZoneTo=WEUR [Accessed 19 November 2020].

[8] H. Psaraftis, C. Kontovas, Speed models for energy-efficient maritime transportation: a taxonomy and survey, Transport. Res. Part C Emerg. Technolog. 26 (2013) 331–351.

[9] M.A. Dulebenets, J. Pasha, O.F. Abioye, M. Kavoosi, Vessel scheduling in liner shipping: a critical literature review and future research needs, Flexible Services Manufact. J. 33 (2021) 43–106.

[10] J. Lam, E. Voorde, Scenario analysis for supply chain integration in container shipping, Maritime Policy Manage. 38 (7) (2011) 705–725.

[11] H. Tai, D. Lin, Comparing the unit emissions of daily frequency and slow steaming strategies on trunk route deployment in international container shipping, Transport. Res. Part D Transport Environ. 21 (2013) 26–31.

[12] D. Lin, Y. Tsai, The ship routing and freight assignment problem for daily frequency operation of maritime liner shipping, Transport. Res. Part E: Logist. Transport. Rev. 67 (2014) 52–70.

[13] A. Zhang, J. Lam, Impacts of schedule reliability and sailing frequency on the liner shipping and port industry: A study of Daily Maersk, Transport. J. 53 (2) (2014) 235–253.

[14] M. Giovannini, H. Psaraftis, The profit maximizing liner shipping problem with flexible frequencies: logistical and environmental considerations, Flexible Services Manufact. J. 31 (2019) 567–597.

[15] M. Moura, M. Pato, A. Paixa, Ship assignment with hub and spoke constraints, Maritime Policy Manage. 29 (2) (2002) 135–150.

[16] J. Álvarez, Joint routing and deployment of a fleet of container vessels, Maritime Economics Logist. 11 (2) (2009) 186–208.

[17] Q. Meng, T. Wang, A chance constrained programming model for short-term liner ship fleet planning problems, Maritime Policy Manage. 37 (4) (2010) 329–346.

[18] S. Gelareh, D. Pisinger, Fleet deployment, network design and hub location of liner shipping companies, Transport. Res. Part E: Logist. Transport. Rev. 47 (6) (2011) 947–964.

[19] Y. Huang, J. Hu, B. Yang, Liner services network design and fleet deployment with empty container repositioning, Comput. Ind. Eng. 89 (2015) 116–124.

[20] J. Zheng, Z. Gao, D. Yang, Z. Sun, Network design and capacity exchange for liner alliances with fixed and variable container demands, Transport. Sci. 49 (4) (2015) 886–899.

[21] K. Thun, H. Andersson, M. Christiansen, Analyzing complex service structures in liner shipping network design, Flexible Serv. Manufact. J. 29 (2017) 535–552.

[22] D. Ronen, The effect of oil price on containership speed and fleet size, J. Operational Res. Soc. 62 (1) (2011) 211–216.

[23] S. Wang, Q. Meng, Robust bunker management for liner shipping networks, Eur. J. Oper. Res. 243 (2015) 789–797.

[24] S. Wang, Q. Meng, Sailing speed optimization for container ships in a liner shipping network, Transport. Res. Part E Logist. Transport. Rev. 48 (3) (2012) 701–714.

[25] H. Kim, A Lagrangian heuristic for determining the speed and bunkering port of a ship, J. Operational Res. Soc. 65 (2014) 747–754.

[26] S. Mander, Slow steaming and a new dawn for wind propulsion: a multi-level analysis of two low carbon shipping transitions, Marine Policy 75 (2017) 210–216.

[27] A. Cheaitou, P. Cariou, Greening of maritime transportation: a multi-objective optimization approach, Ann. Oper. Res. 273 (1–2) (2019) 501–525.

[28] Y. Zhao, J. Zhou, Y. Fan, H. Kuang, Sailing speed optimization model for slow steaming considering loss aversion mechanism, J. Adv. Transport. 2020 (2020) 2157945.

[29] X. Qi, D. Song, Minimizing fuel emissions by optimizing vessel schedules in liner shipping with uncertain port times, Transport. Res. Part E Logist. Transport. Rev. 48 (4) (2012) 863–880.

[30] D. Song, D. Li, P. Drake, Multi-objective optimization for planning liner shipping service with uncertain port times, Transport. Res. Part E Logist. Transport. Rev. 84 (2015) 1–22.

[31] A. Alharbi, S. Wang, P. Davy, Schedule design for sustainable container supply chain networks with port TWs, Adv. Eng. Inf. 29 (2015) 322–331.

[32] Z. Liu, S. Wang, Y. Du, H. Wang, Supply chain cost minimization by collaboration between liner shipping companies and port operators, Transport. J. 55 (3) (2016) 296–314.

[33] M.A. Dulebenets, A comprehensive multi-objective optimization model for the vessel scheduling problem in liner shipping, Int. J. Prod. Econ. 196 (2018) 293–318.

[34] M.A. Dulebenets, Minimizing the total liner shipping route service costs via application of an efficient collaborative agreement, IEEE Trans. Intell. Transp. Syst. 20 (1) (2019) 123–136.

[35] S. Wang, Optimal sequence of container ships in a string, Eur. J. Oper. Res. 246 (3) (2015) 850–857.

[36] S. Gürel, A. Shadmand, A heterogeneous fleet liner ship scheduling problem with port time uncertainty, CEJOR 27 (2019) 1153–1175.

[37] S. Ozcan, D. Eliiyi, L. Reinhardt, Cargo allocation and vessel scheduling on liner shipping with synchronization of transshipments, Appl. Math. Model. 77 (1) (2020) 235–252.

[38] B. Zhang, Z. Zheng, D. Wang, A model and algorithm for vessel scheduling through a two-way tidal channel, Maritime Policy Manage. 47 (2) (2020) 188–202.

[39] D. Zhuge, S. Wang, L. Zhen, G. Laporte, Schedule design for liner services under vessel speed reduction incentive programs, Nav. Res. Logist. 67 (1) (2020) 45–62.

[40] S. Wang, Q. Meng, Container liner fleet deployment: a systematic overview, Transportat. Res. Part C Emerg. Technolog. 77 (2017) 389–404.

[41] J. Pasha, M.A. Dulebenets, M. Kavoosi, O.F. Abioye, O. Theophilus, H. Wang, R. Kampmann, W. Guo, Holistic tactical-level planning in liner shipping: an exact optimization approach, J. Shipping Trade 5 (2020) 1–35.

[42] S. Wang, Q. Meng, Z. Liu, Bunker consumption optimization methods in shipping: a critical review and extensions, Transport. Res. Part C Emerg. Technolog. 53 (2013) 49–62.

[43] C. Kontovas, The green ship routing and scheduling problem (GSRSP): a conceptual approach, Transport. Res. Part D: Transport Environ. 31 (2014) 61–69.

[44] X. Zhao, Q. Lin, H. Yu, An improved mathematical model for green lock scheduling problem of the Three Gorges Dam, Sustainability 11 (9) (2019) 2640.

[45] MAN Diesel & Turbo, 2012. Basic principle of ship propulsion. [online] https://spain.mandieselturbo.com/docs/librariesprovider10/sistemas-propulsivos-marinos/basic-principles-of-ship-propulsion.pdf?sfvrsn=2 [Accessed 24 October 2020].

[46] N. Tran, H. Haasis, T. Buer, Container shipping route design incorporating the costs of shipping, inland/feeder transport, inventory and CO_2 emission, Maritime Economics Logist. 19 (2017) 667–694.

[47] S. Liu, C.A. McMahon, M.J. Darlington, S.J. Culley, P.J. Wild, A computational framework for retrieval of document fragments based on decomposition schemes in engineering information management, Adv. Eng. Inf. 20 (4) (2006) 401–413.

[48] S.W. Hsiao, C.H. Lee, R.Q. Chen, C.Y. Lin, A methodology for brand feature establishment based on the decomposition and reconstruction of a feature curve, Adv. Eng. Inf. 38 (2018) 14–26.

[49] H. Liu, C. Yu, C. Yu, C. Chen, H. Wu, A novel axle temperature forecasting method based on decomposition, reinforcement learning optimization and neural network, Adv. Eng. Inf. 44 (2020), 101089.

[50] OOCL, 2020. Service routes. [online] https://www.oocl.com/eng/ourservices/serviceroutes/Pages/default.aspx [Accessed 24 November 2020].

[51] Ports.com, 2020. Sea route & distance. [online] http://ports.com/sea-route/ [Accessed 24 November 2020].

[52] M.A. Dulebenets, Green vessel scheduling in liner shipping: Modeling carbon dioxide emission costs in sea and at ports of call, Int. J. Transp. Sci. Technol. 7 (1) (2018) 26–44.

[53] Yu, Y., Tu, J., Shi, K., Liu, M., and Chen, J., 2021. Flexible optimization of international shipping routes considering carbon emission cost. Mathematical Problems in Engineering, 2021.